Inorganic Chemistry

Award Paper

pubs.acs.org/IC

Synthetic Cluster Models of Biological and Heterogeneous Manganese Catalysts for O_2 Evolution

Emily Y. Tsui, Jacob S. Kanady, and Theodor Agapie*

Division of Chemistry and Chemical Engineering, California Institute of Technology, Pasadena, California 91125, United States

ABSTRACT: Artificial photosynthesis has emerged as an important strategy toward clean and renewable fuels. Catalytic oxidation of water to O_2 remains a significant challenge in this context. A mechanistic understanding of currently known heterogeneous and biological catalysts at a molecular level is highly desirable for fundamental reasons as well as for the rational design of practical catalysts. This Award Article discusses recent efforts in synthesizing structural models of the oxygen-evolving complex of photosystem II. These structural motifs are also related to heterogeneous mixed-metal oxide catalysts. A stepwise synthetic methodology was developed toward achieving the structural complexity of the targeted active sites. A geometrically restricted multinucleating ligand, but with labile coordination modes, was employed for the synthesis of low-oxidation-state trimetallic species. These precursors were elaborated to site-differentiated tetrametallic complexes in high oxidation states. This methodology has allowed for structure−reactivity studies that have offered insight into the effects of different components of the clusters. Mechanistic aspects of oxygen-atom transfer and incorporation from water have been interrogated. Significantly, a large and systematic effect of redox-inactive metals on the redox properties of these clusters was discovered. With the pK_a value of the redox-inactive metal−aqua complex as a measure of the Lewis acidity, structurally analogous clusters display a linear dependence between the reduction potential and acidity; each pK_a unit shifts the potential by ca. 90 mV. Implications for the function of the biological and heterogeneous catalysts are discussed.

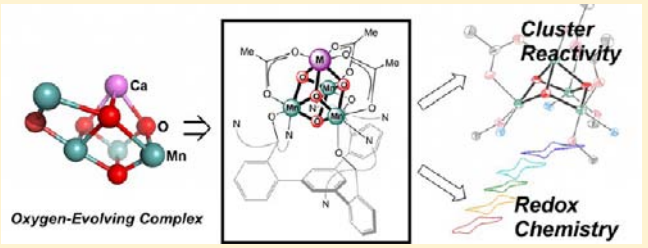

1. INTRODUCTION

Photosynthesis, the sunlight-powered process by which plants, algae, and cyanobacteria convert carbon dioxide and water into carbohydrates and dioxygen (O_2), is responsible for the O_2 in the Earth's atmosphere.[1−3] Light-driven water oxidation occurs at photosystem II (PSII), a membrane protein assembly that absorbs four photons to sequentially oxidize a $CaMn_4O_5$ cluster, known as the water-oxidizing complex or the oxygen-evolving complex (OEC), through a sequence of S_n states called the Kok cycle.[4,5] At the most oxidized state, S_4, O_2 is released. Water acts as the source of the electrons that are transferred through a series of cofactors and stored as NADPH.[1−3] The reducing equivalents and proton gradient generated by photochemical water oxidation power carbon dioxide fixation and other processes of life. Overall, solar energy is converted and stored as chemical bonds. Many efforts have been devoted to structural, spectroscopic, and biochemical studies of the OEC because understanding how plants form oxygen from water will have implications for designing artificial catalysts for solar fuels. Heterogeneous metal oxide water oxidation catalysts have been proposed to perform their function at discrete multimetallic sites reminiscent of the OEC.[6−10] Artificial water oxidation catalysts have been prepared from calcium-doped manganese oxide materials to mimic the composition of the OEC, despite the limited structural understanding.[8,11−14] Other mixed-metal oxides have intriguing catalytic properties for both water oxidation and oxygen reduction.[15−19] Metal oxides are also important as battery materials.[20−23] Access to and the study of well-defined metal oxide clusters structurally analogous to the active sites of these catalysts are expected to provide insight into the interactions between different types of metals and their effects on the properties of the cluster and catalytic material.

1.1. Structural and Mechanistic Studies of the OEC.

X-ray absorption spectroscopy (XAS)[24−28] and electron paramagnetic resonance (EPR)[29−34] methods have been employed to identify oxidation state, electronic structure, and coordination environment changes during the *S*-state progression. Recent single-crystal X-ray diffraction (XRD) studies have shown that the OEC consists of a $CaMn_3O_4$ cubane cluster with the fourth "dangler manganese" center bridged via oxide moieties (Figure 1).[35,36] Subsequent computational studies, however, have suggested that this structure corresponds to a more reduced manganese cluster due to X-ray damage,[37,38] consistent with previous studies on X-ray-induced reduction,[39] or to an equilibrium of multiple structural forms at similar energies.[40,41] More open cubane structures of the S_2 state have been proposed by calculations that are consistent with OEC geometries advanced from EPR and XAS studies (Figure 2).[28,31,41−43]

Because of these uncertainties in the structural details of the *S* states of the OEC, the mechanism of O−O bond formation during water oxidation remains controversial. Isotopic-labeling studies using mass spectrometry and magnetic resonance

Received: September 2, 2013
Published: December 16, 2013

   dx.doi.org/10.1021/ic402236f | *Inorg. Chem.* 2013, 52, 13833−13848

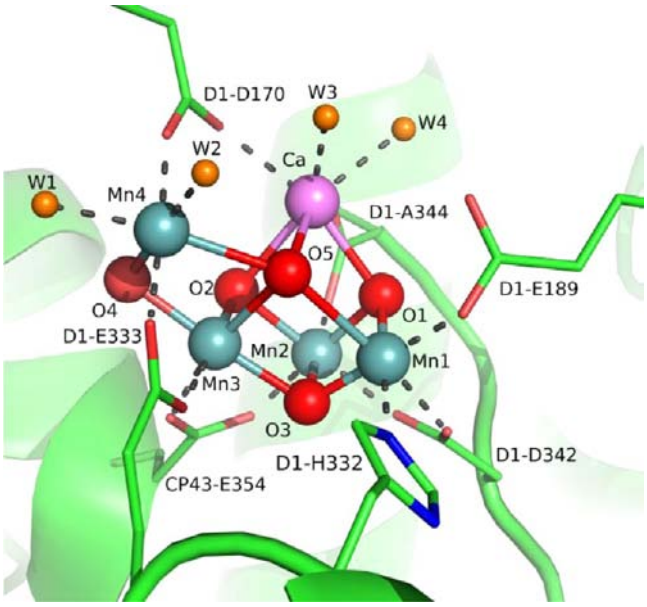

Figure 1. Structure of the OEC from single-crystal XRD studies.[36]

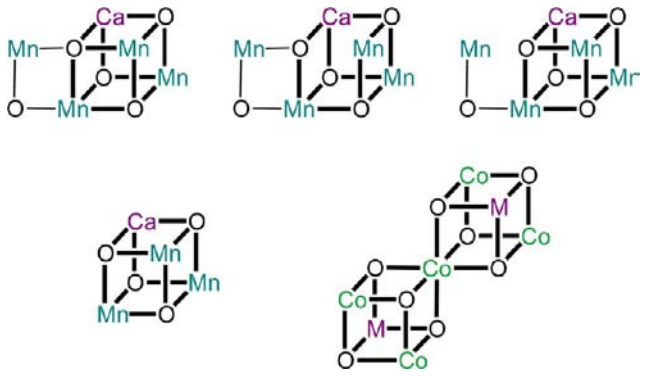

Figure 2. Proposed structure of the OEC from single-crystal XRD studies (top left)[35,36] and more open structures proposed from XAS and computational studies (top middle, right).[40,41] Proposed structure of the catalytic sites in calcium-doped manganese oxide water oxidation catalysts (bottom left)[8,9] and of cobalt oxide water oxidation catalysts (bottom right).[6]

techniques have been used to analyze substrate water exchange rates with bulk water within the OEC.[44−46] On the basis of these studies and spectroscopic data, several mechanisms for O−O bond formation have been proposed. These proposals differ in the nature and location of the substrate oxo moieties that undergo O−O bond formation to generate O_2. Early proposals, such as the manganese-only adamantane and the double-pivot mechanisms, proved incorrect based on structural grounds.[47−49] Heterolytic pathways involve a water or hydroxide ligand bound to Ca^{2+} attacking a manganese(V) oxo or manganese(IV) oxyl.[50−52] Other mechanisms have suggested that a terminal oxyl reacts with a bridging oxido moiety via a radical mechanism (Figure 3).[42,53,54] Distinguishing the different mechanisms through computational and experimental studies remains a challenge.

The role of calcium, which is known to be necessary for activity, is an unclear aspect of water oxidation at the OEC.[57−60] In particular, the association of Ca^{2+}, a redox-inactive metal, with an active site that performs a multielectron redox transformation is puzzling and departs from other roles of Ca^{2+} in

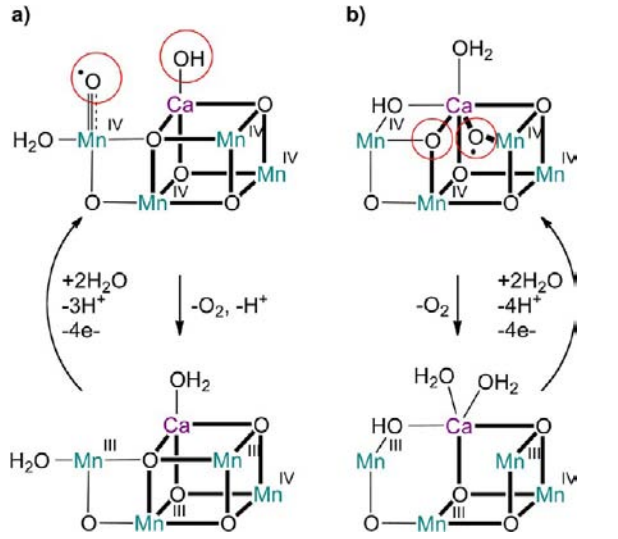

Figure 3. Recent proposed mechanisms of O−O bond formation in the OEC,[50,55,56] with sites of substrate incorporation highlighted in red.

biological systems. XAS and XRD studies have revealed that Ca^{2+} is bridged by oxido moieties to the manganese centers in the OEC but does not function solely as a structural component. Substitution of other metal ions for Ca^{2+} leads to inhibition of catalysis, except for Sr^{2+}, which recovers activity, albeit to a lower extent (ca. 40%).[3,57,61] The Sr^{2+}-substituted OEC shows subtle changes in geometry (XAS)[62] and electronic structure (EPR)[63] compared to the native $CaMn_4O_x$ cluster. The ability of Sr^{2+} and Ca^{2+} to maintain catalysis has been explained in terms of their similar Lewis acidities in the context of binding and activating a water substrate.[50,52,64,65] Size or charge effects were deemed secondary because Cd^{2+}, an ion with the same ionic radius as Ca^{2+}, does not support water oxidation.[3,64] Others have proposed that Ca^{2+} affects proton-coupled electron transfer and the redox properties of the cluster, possibly via interactions through a hydrogen-bonding network with the neighboring tyrosine residue or by affecting the protonation state of a coordinated water molecule.[26,66,67] Despite detailed biochemical and spectroscopic studies, the role of calcium in the OEC remains under debate. Synthetic models to complement these investigations were extremely scarce and not structurally accurate, until recently.

1.2. Heterogeneous Metal Oxides as Water Oxidation Catalysts. Heterogeneous manganese-containing materials have been studied for their water oxidation activities, and parallels have been drawn to the biological system. Although undoped manganese oxides have been demonstrated to catalyze water oxidation at low efficiencies, the addition of calcium greatly increases the reaction efficiency, raising the possibility that the mechanism of O_2 formation is related to that of the biological OEC.[11,14] XAS studies of these materials determined that the manganese centers are of the 3+ and 4+ oxidation states and that the redox-inactive ions may be bridged to the manganese centers by oxido moieties in MMn_3O_4 cuboidal subsites similar to those in the OEC.[8,9] These results suggest that a further understanding of PSII may allow for the rational design of more efficient heterogeneous water oxidation catalysts. Beyond manganese water oxidation catalysts, the proposed catalytic site of cobalt oxide has been illustrated with redox-inactive cations at positions reminiscent of the Ca^{2+}

dx.doi.org/10.1021/ic402236f | Inorg. Chem. 2013, 52, 13833−13848

position in the OEC (Figure 2)[6,7] [although alkaline metals were not detected by extended X-ray absorption fine structure (EXAFS)].[68]

1.3. Synthetic Manganese Clusters. Synthetic biomimetic complexes have been targeted to supplement the structural, spectroscopic, and mechanistic studies of biological systems while at the same time exploring the possibilities of catalysis. Structural and functional modeling of the OEC has been challenging, in particular because of the propensity of the oxido moieties to bridge and generate oligomeric structures in an uncontrolled fashion. Many mononuclear, dinuclear, trinuclear, and tetranuclear manganese complexes have been prepared as models and have been extensively reviewed in the literature.[2,69−78] These high-oxidation-state manganese oxido complexes are often synthesized by spontaneous self-assembly by oxidation of manganese(II) salts; for these compounds, the choice of oxidant is crucial. Bridging oxides are known to stabilize higher-oxidation-state manganese centers but also to significantly affect the geometry, Mn−Mn distance, and magnetic exchange of these compounds.[69] A second important aspect is the choice of ancillary ligands. These ligands, often polydentate oxygen or nitrogen donors, are chosen to limit aggregation and to stabilize certain oxidation states. Manganese carboxylate chemistry especially has been heavily studied because of the carboxylate-containing residues in the OEC binding site.[72] In the following section, selected examples of manganese oxide clusters will be discussed, with emphasis on tetramanganese and heterometallic complexes because they are particularly relevant to the composition of the OEC.

Mixed-valent dimanganese(III,IV) bis(μ-oxo) dimers stabilized by polydentate nitrogen-donor ligands have been of particular interest in OEC biomimetic chemistry since they were first prepared and studied for their magnetic exchange coupling properties (Figure 4, **A**).[79−81] Although these lower-nuclearity complexes were clearly not structural mimics of the tetramanganese OEC cluster, they were heavily studied because of the Mn−Mn distance of 2.7 Å, which is similar to distances in the OEC measured by XAS studies,[82] as well as a multiline EPR signal that is similar to the multiline signal observed for the S_2 state of the OEC.[81,83] From a structural perspective, a dimer-of-dimers model was proposed for the S_2-state OEC based on these observations,[26,84] and synthetic models were prepared (Figure 4, **B**).[85−87] The dimer-of-dimers model was later shown to be inconsistent with EPR spectroscopic measurements that support a 3 + 1 arrangement of the manganese centers.[31] From a functional aspect, Brudvig and co-workers have used a terpyridine-supported dimanganese(III,IV) bis(μ-oxo) complex for water oxidation using oxone or hypochlorite as the oxidant.[88,89] On the basis of kinetic and isotopic-labeling studies, a terminal $Mn^{V}O$ moiety was proposed as an intermediate for O_2 formation.[90]

One of the earliest high-oxidation-state tetramanganese oxido clusters, prepared by Christou and co-workers, was a $[Mn_4O_2]$ complex in which the manganese centers are in a "butterfly" arrangement (Figure 4, **C**).[91,92] This structure was proposed to participate in the Kok cycle through a "double-pivot" mechanism to rearrange to more cubane-like structures.[48] Tetramanganese cubane structures had previously been proposed as intermediates in the water oxidation pathway of the OEC[48,49] but were not synthetically accessed until Christou and co-workers isolated an acetate-bridged tetramanganese trioxido chloride cubane complex (Figure 4, **D**).[93] A diarylphosphinate-supported tetraoxido $[Mn_4O_4]^{n+}$ cubane variant

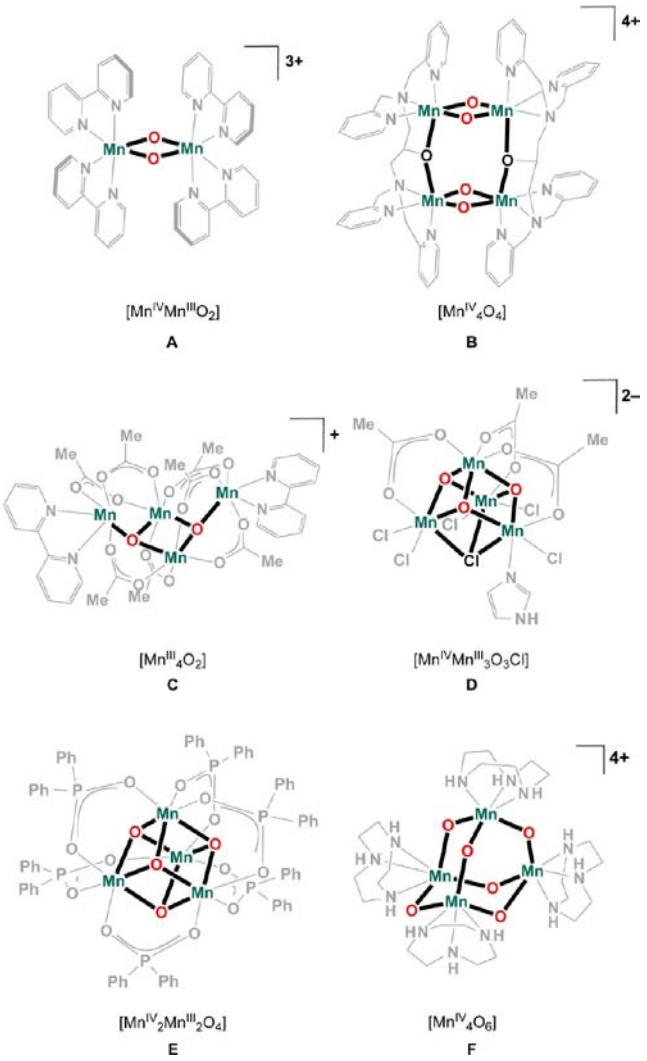

Figure 4. Selected examples of di- and tetramanganese oxido clusters.[79,85,92−94,98]

was later isolated by Dismukes and co-workers via the spontaneous assembly of mononuclear or dinuclear manganese precursors (Figure 4, **E**).[94,95] These clusters are proposed to be stabilized by π interactions between the aryl groups of the phosphinate ligands.[95] The diarylphosphinate-stabilized system was also proposed to photoelectrochemically oxidize water to O_2 when embedded in a Nafion film;[96] however, an amorphous manganese oxide material was later found to be the active catalyst.[97] Adamantane-type tetramanganese clusters have also been described (Figure 4, **F**).[98,99]

One of the most important, but least explored, problems in preparing accurate structural models of the OEC has been the incorporation of calcium into the clusters. Heterometallic manganese clusters are relatively rare and have been isolated as molecular species only in recent years.[100−106] The first high-oxidation-state manganese cluster with incorporated calcium, $[Mn_{13}Ca_2O_{10}(OH)_2(OMe)_2(O_2CPh)_{18}(H_2O)_4]\cdot 10MeCN$ (Figure 5, **G**) was prepared by Christou and co-workers from calcium salts such as $Ca(NO_3)_2\cdot 4H_2O$, $Ca(ClO_4)_2$, or $Ca(O_2CPh)_2$ and $(NBu_4)[Mn_4O_2(O_2CPh)_9(H_2O)]$.[100] Although this is a high-nuclearity $[Mn_{13}Ca_2]$ cluster much larger than the $[Mn_4Ca]$ motif found in PSII, one portion resembled the OEC in that it had a $CaMn_3O_4$ cubane subunit

dx.doi.org/10.1021/ic402236f | Inorg. Chem. 2013, 52, 13833−13848

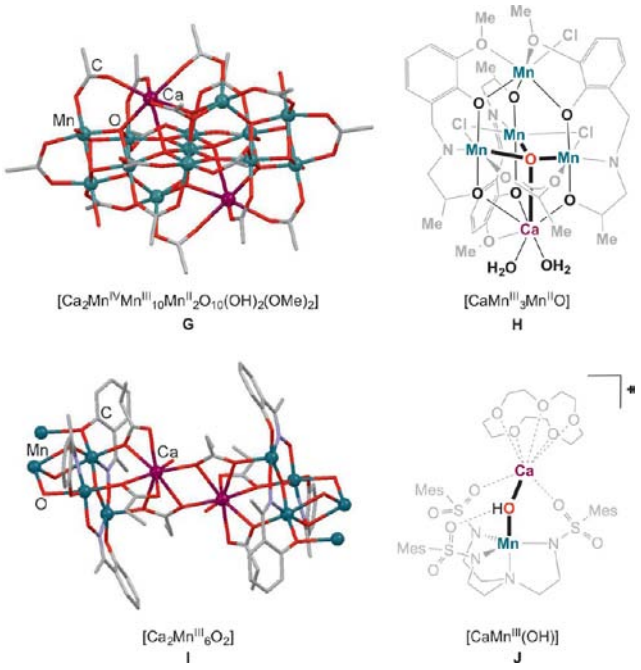

Figure 5. Structurally characterized heterometallic calcium/manganese clusters with bridging oxide or hydroxide moieties.[100,102,104,108]

with a fourth manganese center bridged to the cluster via an oxide moiety. A similar compound with Sr^{2+} rather than Ca^{2+} was also later isolated and studied.[101,107] Powell and co-workers used a chelating Schiff base ligand to generate $CaMn_4$ clusters, although with only one incorporated oxide moiety (Figure 5, **H**).[102,103] A heterometallic polymeric material with a Mn_3O unit in proximity to a Ca^{2+} center was isolated (Figure 5, **I**).[108] To the authors' knowledge, only three other manganese/calcium clusters had been reported and characterized by crystallography prior to 2011, all with no bridging oxido ligands: a Mn_4 metallacrown moiety with a Ca^{2+} center coordinated to one side of the crown and chelated by carboxylates;[109] a $Mn^{II}_4Ca_2$ cluster with bridging alkoxides;[110] a Mn_3NaCa coordination polymer.[111] The oxidation state of manganese in these compounds varies from mixed-valent $Mn^{II}/Mn^{III}/Mn^{IV}$ or Mn^{II}/Mn^{III} to all-Mn^{II} or all-Mn^{III}. These synthetically novel heterometallic compounds demonstrate that although the self-assembly strategy is structurally very versatile, control of the oxidation state, oxide incorporation, and level of aggregation to form the desired molecular model clusters remains challenging.

A complementary approach reported concurrently with our work on clusters investigated the effects of Ca^{2+} and other redox-inactive metals in heterometallic binuclear complexes. Borovik and co-workers exploited a tripodal tris(sulfonamide) ligand framework to access complexes of transition metals such as manganese, iron, and cobalt associated via a bridging hydroxide with Ca^{2+}, Sr^{2+}, and Ba^{2+} centers that are also coordinated by two sulfonamide oxygen donors (Figure 5, **J**).[104,106,112] The redox-inactive metal was reported to affect the reduction potentials of the complexes as well as the rate of reaction with O_2. Although not structurally characterized, Sc^{3+} association to $Mn^{IV}O$ moieties has been reported by Fukuzumi, Nam et al. to affect the reduction potential as well as reactivity, including the rates of electron transfer, oxygen-atom transfer, and hydrogen-atom abstraction.[113,114] Related effects have been observed for $Fe^{IV}O$ moieties coordinated with redox-inactive metals, with the Sc^{3+} version being structurally characterized.[115,116] Valence tautomerism was reported by Goldberg, de Visser, et al. for $Mn^{V}O$ porphyrinoid complexes upon the addition of Zn^{2+}, which affected redox- and hydrogen-atom-transfer chemistry.[117] These elegant studies show clearly that redox-inactive metals significantly affect the chemistry of transition-metal oxo species. Implications to the chemistry of the OEC have been proposed; however, more structurally accurate cluster models of the OEC remain very desirable to interrogate the effects on the physical properties and chemical reactivity of the complexes by changing various aspects such as the structure, oxidation state, nature of the redox-inactive metal, and number of oxido moieties.

2. SYNTHESIS OF SITE-DIFFERENTIATED MULTINUCLEAR MANGANESE COMPLEXES

Access to models of the active sites in biological and heterogeneous catalysts for water oxidation represents a significant synthetic challenge for several reasons, including the relatively large number of atoms, the presence of two types of metals, metal lability, and cluster asymmetry. In one possible strategy for modeling the OEC, outlined in a retrosynthetic fashion (Scheme 1), the "dangler" is attached late in the synthesis to a

Scheme 1. Retrosynthetic Analysis for the Synthesis of an OEC Model

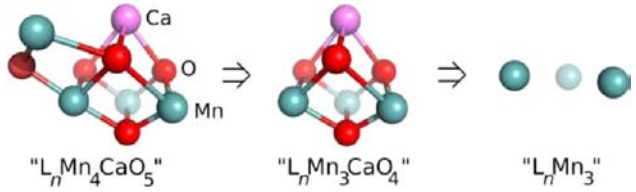

$CaMn_3O_4$ cubane structure. Accessing the simpler and higher-symmetry $CaMn_3O_4$ cubane presents the challenge (vide supra) of incorporating two types of metals bridged by oxides in the same cluster in a 3:1 ratio. A precursor to such species was envisioned in a trimetallic manganese complex.

This synthetic approach is reminiscent of Holm's methodology for the preparation of site-differentiated cuboidal iron/sulfur clusters.[118−122] Site-differentiated Fe_4S_4 cubanes are found in several metalloenzymes, with one of the supporting cysteinyls bridged to another metal fragment. In order to model such moieties, a semirigid tris(thiolate) ligand was employed to support three of the four metals of the cubane moiety. Incomplete iron/sulfur clusters, Fe_3S_4, supported by this trinucleating ligand could be isolated and utilized as precursors to homo- and heterometallic Fe_3MS_4 moieties (Scheme 2).

Toward heterometallic manganese oxido complexes, preformed trimanganese clusters were targeted that could be oxidized with the concomitant addition of a fourth metal center. A multinucleating ligand based upon a semirigid 1,3,5-triarylbenzene framework was synthesized, with the three peripheral aryl groups functionalized by a dipyridylmethanol moiety (Scheme 3). The lability of the dipyridylalkoxymethyl moiety is well documented in the coordination chemistry of dipyridylketone and the *gem*-diol or hemiacetal form thereof, which chelate and bridge metal ions in a wide variety of binding modes.[123] Such coordinative flexibility was expected to support the formation of different types of clusters on the ligand architecture. Additionally, these donor moieties were expected

dx.doi.org/10.1021/ic402236f | Inorg. Chem. 2013, 52, 13833−13848

Scheme 2. Metal Incorporation into Subsite-Differentiated Fe_3MS_4 Clusters[122]

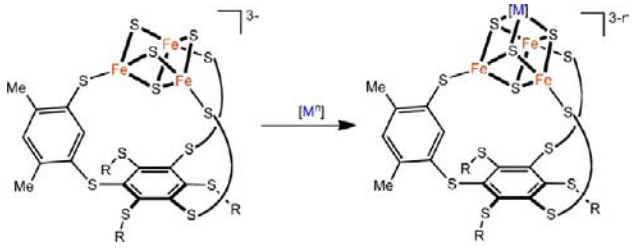

Scheme 3. Synthesis of Trimetallic Complexes $LM^{II}_3(OAc)_3$ (1; M = Mn)

to support high-oxidation-state metal centers and be relatively stable to oxidative reaction conditions.

Ligand H_3L (Scheme 3) was prepared on a multigram scale in two synthetic steps from commercially available materials. Lithium−halogen exchange of 1,3,5-tris(2′-bromophenyl)-benzene, prepared by cyclization of 2-bromoacetophenone, followed by the addition of 3 equiv of di-2-pyridylketone affords H_3L in approximately 40% yield over two steps. Compound H_3L was treated with divalent transition-metal salts (M^{2+} = Mn^{2+}, Fe^{2+}, Co^{2+}, Ni^{2+}, Cu^{2+}, Zn^{2+}) in the presence of base to form trinuclear complexes. The solid-state structures of these compounds show that the ancillary-functionalized triarylbenzene ligand binds the three metal centers in the same fashion, independent of the nature of the metal. The three metals are bridged by μ-alkoxides and pyridyl groups from each arm of the ligand framework coordinated to adjacent metals (Scheme 3; Figure 6).[124,125] Notably, these complexes are stable in the presence of water. Except for the zinc complex, these complexes all have paramagnetically shifted ^{1}H NMR spectra with diagnostic peaks that allow monitoring of the reaction progress and identification of the target products. The trinuclear clusters are capped by the counterions from the initial metal salts. The trimanganese(II) tris(acetate) compound $LMn_3(OAc)_3$ (**1**) was selected as a starting platform for further oxidative functionalization. Compound **1** provides three manganese(II) centers poised for oxidation and proximally constrained by the ligand framework and bridging alkoxide moieties; furthermore, the acetate ions can serve as ancillary ligands to bridge to additional metal centers.

2.1. Synthesis of Mn_4O_x Complexes. The oxidative incorporation of a fourth metal into **1** was studied with various manganese precursors targeting tetramanganese clusters. In this context, permanganate can act as the source of the fourth metal equivalent and oxide moieties and as the oxidant. The treatment of **1** with 2 equiv of ^{n}Bu$_4$NMnO$_4$ leads to isolation of a tetramanganese tetraoxido cubane cluster, $LMn^{III}_2Mn^{IV}_2O_4(OAc)_3$ (**2**) in 30% isolated yield (Scheme 4 and Figure 7).[126]

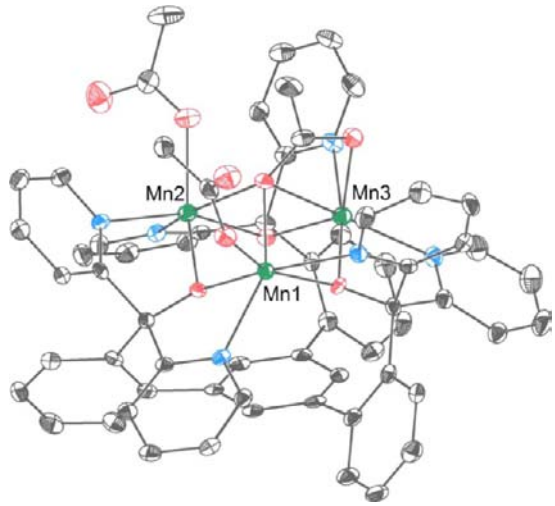

Figure 6. Solid-state structure of **1**.

The relatively low yield is likely due to the unbalanced nature of the reaction.

Complex **2** contains a Mn_4O_4 cubane unit, with the overall charge and bond lengths consistent with the $Mn^{III}_2Mn^{IV}_2$ oxidation state. To accommodate such a drastic change in the cluster structure, the acetates and dipyridylalkoxide units change binding modes from those observed in **1**. The alkoxides shift from bridging to terminal coordination, three of the pyridyl donors decoordinate, and the three acetates form κ^2-bridges across three cubane faces. Complex **2** is pseudo-C_3-symmetric. One previous class of Mn_4O_4 cubane complexes with only μ_3-oxido donors has been isolated (**E**), supported by diarylphosphinate bridging ligands.[94] Christou and co-workers studied extensively $Mn^{III}_3Mn^{IV}O_3X$ cubanes (X = Cl^-, I^-, F^-, N_3^-, O_2CR^-, OMe^-, OH^-).[127−131]

With **1** as the precursor, separation of the oxidizing and oxygen equivalents from the metal source was explored, thus expanding the parameter space and providing access to a wider range of tetrametallic complexes. Using potassium superoxide as the oxidant and oxygen source while varying the manganese salt—$Mn(OAc)_2$ versus $Mn(OTf)_2$—and solvent afforded a series of tetramanganese complexes varying in the oxido content and oxidation state from μ_4-oxido $Mn^{II}_3Mn^{III}O$ (**3**) and $Mn^{II}_2Mn^{III}_2O$ (**4**) complexes to a dioxido complex $Mn^{II}_2Mn^{III}_2O_2$ (**5**) and partial cubane complex $Mn^{III}_4O_3$ (**6**; Scheme 4 and Figure 7).[132]

In **3** and **4**, the ligand framework coordinates three manganese centers as in **1**, but now a μ_4-oxido and three acetates bridge the three basal manganese centers to a fourth five-coordinate manganese center (Figure 7). The tetrahedral μ_4-oxido is a common motif throughout manganese cluster chemistry[76] and is also a common motif in our work with the L^{3-} framework. For dioxido complex **5**, a μ_4-oxido bridges the four manganese centers as in **3**. Additionally, a second μ_2-oxido bridges one basal manganese and the apical manganese, forming a $Mn^{III}_2O_2$ diamond core. Complex **5** reacts with O_2, formally reducing it by four electrons over days to generate cubane complex **2**, indicating that O_2 reactivity is possible in these systems. For complex **6**, as the oxido content increases from 2 to 3, the binding mode of L^{3-} changes to that of **2**, with terminal alkoxides and only three coordinated pyridines. A comparison of the electrochemical properties of **2** and **6** shows one oxidation and one reduction event for each,

dx.doi.org/10.1021/ic402236f | Inorg. Chem. 2013, 52, 13833−13848

Scheme 4. Synthesis and Interconversion of Tetramanganese Complexes 2−7

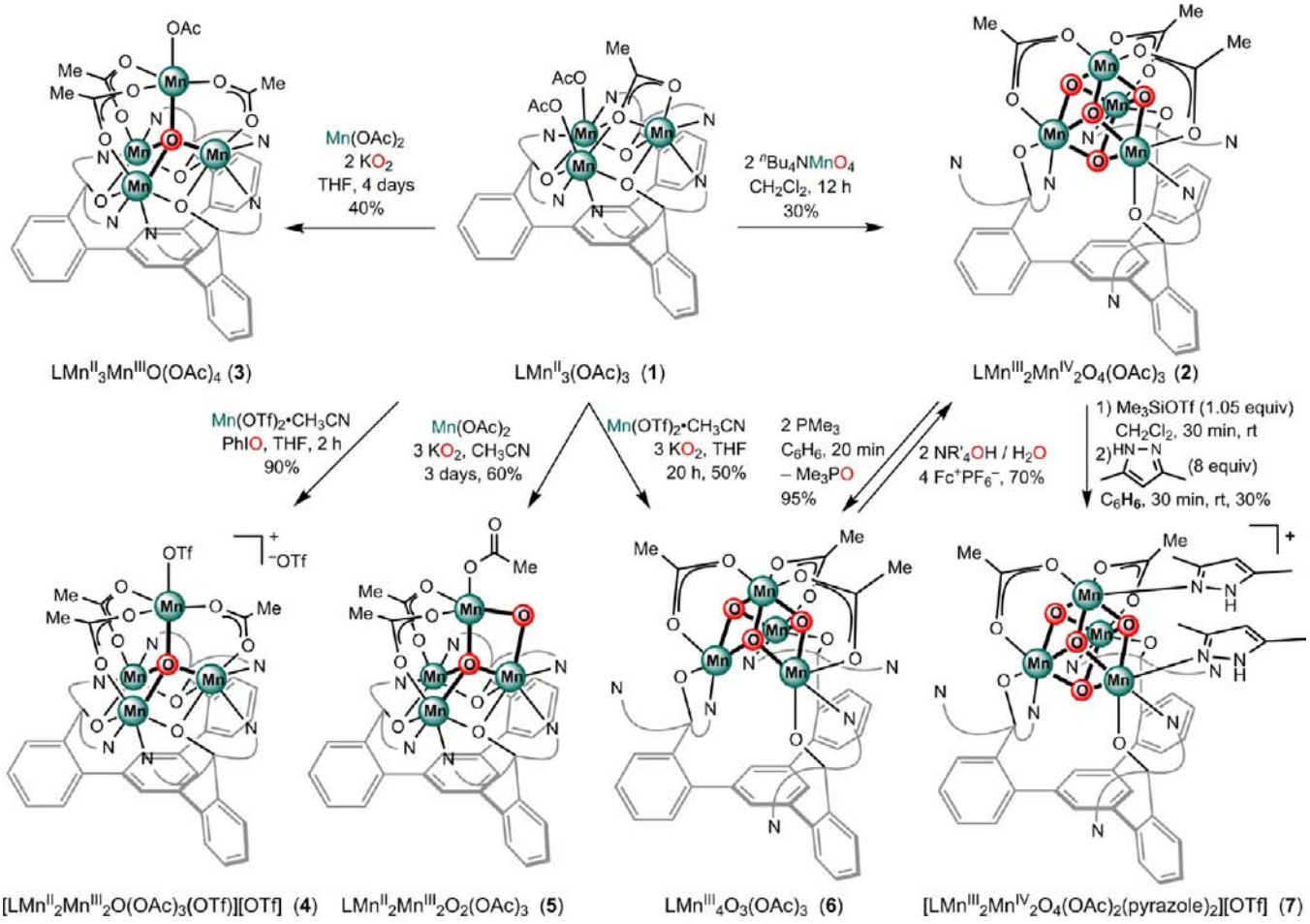

with differences of less than 150 mV between the two compounds, despite a difference of two units between the metal oxidation states of the two species. This behavior results from neutralization of charge buildup on the cluster by incorporation of an O^{2-} donor.[133] This redox leveling of the cluster upon formal water incorporation and deprotonation is relevant to the OEC because the oxidizing equivalents come at the same potential for all four oxidations during catalysis to generate O_2.

Cationic $Mn^{III}_2Mn^{IV}_2$ cubane complexes such as **7** were prepared by the reaction of **2** with 1 equiv of trimethylsilyl triflate, followed by the addition of neutral Lewis bases. Such lower-symmetry species, which have one of the Mn_2O_2 faces of the cubane free of anionic ligands, are synthetically important toward accessing clusters with a fifth dangling metal similar to the OEC.

Complexes **2**−**6** span six oxidation states, with two more—Mn^{II}_4 and $Mn^{III}Mn^{IV}_3$—accessible electrochemically. The ability of the present multinucleating ligand architecture to support different binding modes is instrumental for accessing the wide span of metal oxidation states and oxido contents. Clusters displaying low-oxidation-state Mn^{II} centers are coordinated by 9 donors from L, binding to 12 coordination sites (counting three μ-alkoxides) while the higher-oxidation-state species, displaying Mn^{III} and Mn^{IV}, require only six donors (Figure 8). The switch in the coordination mode is likely due to the strong manganese−oxido bonds that lead to the displacement of the pyridine and μ-alkoxide donors. The present compounds suggest that donor flexibility is an important factor in the design of ligands for clusters in multielectron chemistry involving transfers of oxygenous moieties. Although the binding mode varies, the ligand set changes little other than the inclusion of oxido ligands, paralleling the photoassembly of the OEC, from four free Mn^{II} ions to the active Mn_4CaO_x cluster.

2.2. Synthesis of $CaMn_3O_x$ Complexes. To access heterometallic complexes structurally related to the OEC, calcium/manganese oxido clusters of various oxidation states and oxido contents were prepared using an approach similar to that used for homometallic complexes **3**−**6**. The triflate salt was employed as the source of Ca^{2+}, and PhIO or superoxide was used as the source of oxygen and oxidizing equivalents. The treatment of a tetrahydrofuran (THF) mixture of **1** and $Ca(OTf)_2$ with PhIO forms the purple compound $[LMn_3O(OAc)_3]_2Ca(OTf)_2$ (**8**), in which each trimanganese moiety has been oxidized to form a $[Mn^{III}_2Mn^{II}O]$ cluster; two $[Mn^{III}_2Mn^{II}(\mu_3\text{-}O)]$ moieties are bridged by acetate ligands to a calcium center that has no interaction with the oxido group (Scheme 5).[126] In the structure of **8**, as in compounds **1** and **3**−**5**, the alkoxide moieties of the multinucleating ligand framework bridge the manganese centers in the basal trimanganese core, and all pyridyl donors are coordinated. Isolation of **8** demonstrated the viability of our strategy of oxidative functionalization of **1** with nonmanganese metal sources. More oxidized complexes, relevant to the oxidation states proposed for the *S* states formed during the Kok cycle, were targeted.

The treatment of **8** with 1 equiv of $Ca(OTf)_2$ and 2 equiv of PhIO in 1,2-dimethoxyethane (DME) forms the dioxido

dx.doi.org/10.1021/ic402236f | *Inorg. Chem.* 2013, 52, 13833−13848

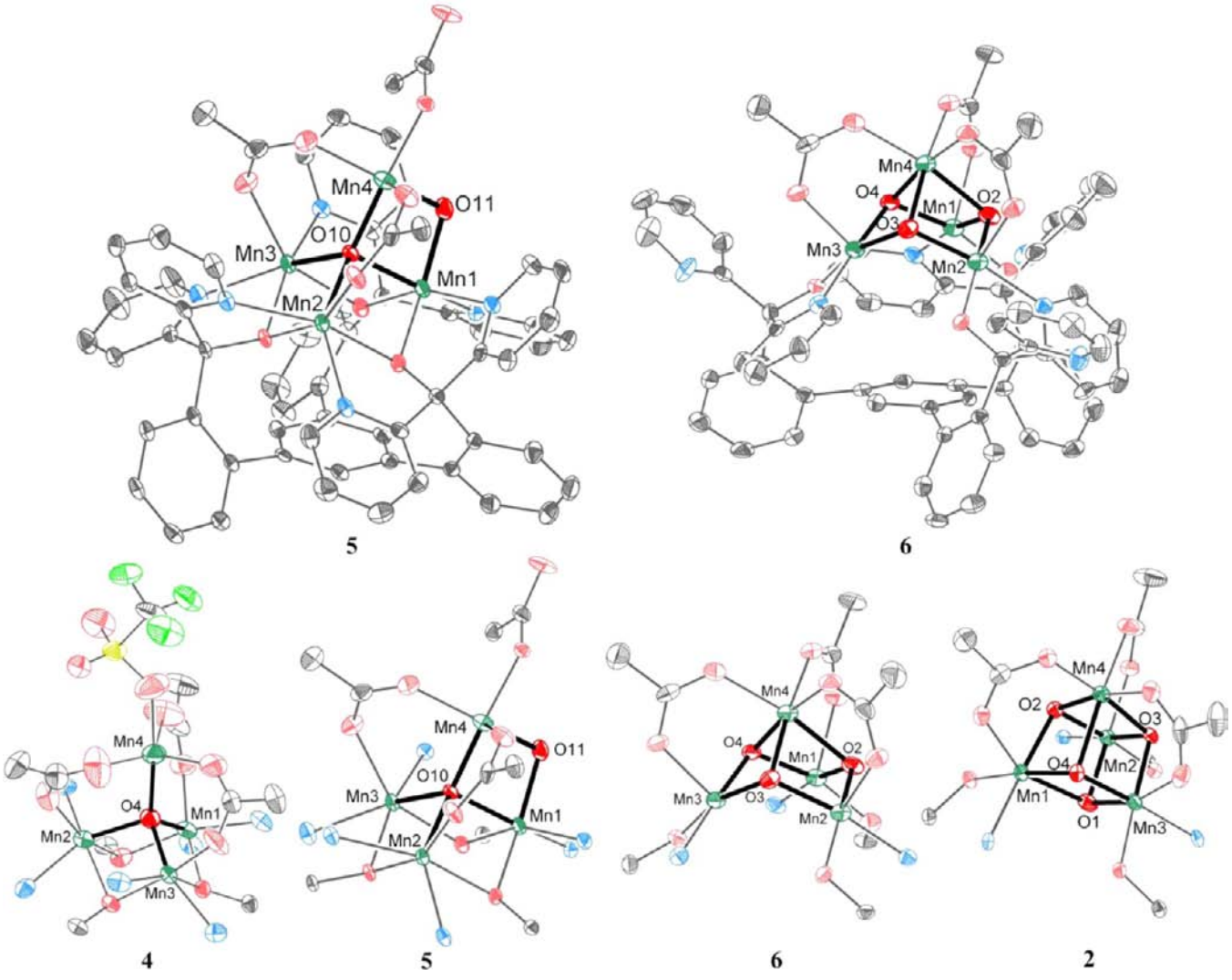

Figure 7. Solid-state structures of tetramanganese complexes **2**–**6**.

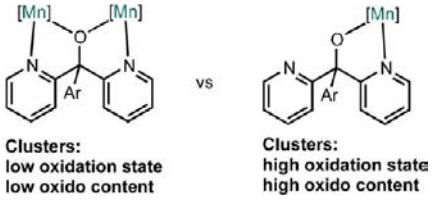

Figure 8. Ligand flexibility as a function of the cluster oxido content and oxidation state: binding modes of dipyridylalkoxide arms.

complex $[LCaMn^{III}_2Mn^{IV}O_2(OAc)_2(DME)(OTf)][OTf]_2$ ($[\mathbf{9}\text{-}Ca(DME)(OTf)][OTf]_2$; Scheme 5).[134] Compound $[\mathbf{9}\text{-}Ca(DME)(OTf)][OTf]_2$ can also be prepared directly from **1** by treatment with $Ca(OTf)_2$ (1.5 equiv) in DME with PhIO (2 equiv). In $[\mathbf{9}\text{-}Ca(DME)(OTf)][OTf]_2$, the Ca^{2+} center is bridged to the more oxidized $[Mn^{IV}Mn^{III}_2]$ unit via two acetate ligands as well as bridging μ_2- and μ_4-oxido moieties (Figure 9, left). The Ca^{2+} center is further coordinated by a DME ligand and a κ_1-trifluoromethanesulfonate anion, with two triflate anions remaining outer sphere. The DME and triflate ligands on Ca^{2+} can be substituted with other donors. For example, upon exposure to water, the tris(aqua) variant $[\mathbf{9}\text{-}Ca(OH_2)_3]^{3+}$ was isolated and structurally characterized (Figure 9, right). Compound $[\mathbf{9}\text{-}Ca(DME)(OTf)][OTf]_2$ reacts with decamethylferrocene ($FeCp^*_2$) to generate the isostructural one-electron-reduced Mn^{III}_3 compound $[\mathbf{10}\text{-}Ca(DME)(OTf)][OTf]$. The coordination environments of complexes $[\mathbf{10}\text{-}Ca(DME)(OTf)]^+$ (Mn^{III}_3) and $[\mathbf{9}\text{-}Ca(DME)(OTf)]^{2+}$ ($Mn^{III}_2Mn^{IV}$) are identical, with only slight changes in the bond lengths due to changes in the oxidation state at manganese. The treatment of $[\mathbf{10}\text{-}Ca(DME)(OTf)][OTf]$ with AgOTf regenerates $[\mathbf{9}\text{-}Ca(DME)(OTf)][OTf]_2$. Compounds **9** and **10** are structurally related to the tetramanganese dioxido complex **5** but with more oxidized manganese centers.

To form a more oxidized $CaMn_3$ cluster in analogy to the formation of the all-manganese clusters **2** and **7**, a mixture of **1** and $Ca(OTf)_2$ was treated with excess KO_2 in THF/DME mixture to afford a tetraoxido cubane compound $LCaMn^{IV}_3O_4(OAc)_3(THF)$ (**11**-Ca). Compound **11**-Ca can also be isolated by the oxidation of $[\mathbf{9}\text{-}Ca(DME)(OTf)]^{2+}$ with sodium peroxide or the oxidation of **8** with potassium superoxide, indicating that these partially oxidized species could be intermediates on the path to generating the cubane from low-oxidation-state precursors, as in biological photoactivation. The structure of **11**-Ca is closely related to that of **2**, with four μ_3-oxido moieties bridging the four metals, although **11**-Ca is more oxidized than **2** and contains three manganese(IV) centers. As with **2**, the coordination mode of the alkoxide

dx.doi.org/10.1021/ic402236f | *Inorg. Chem.* 2013, 52, 13833–13848

Scheme 5. Synthesis of $CaMn_3O_x$ Clusters

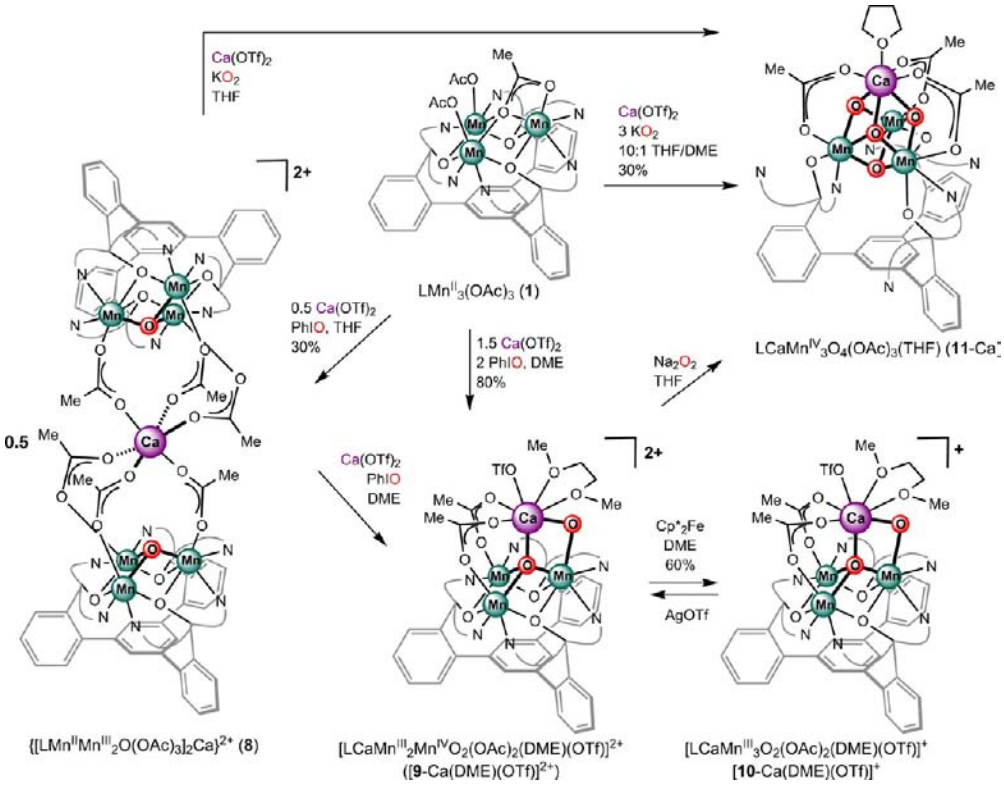

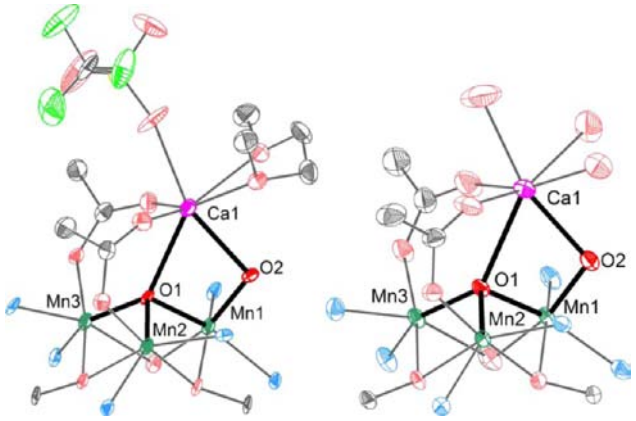

Figure 9. Truncated solid-state structures of $[\mathbf{9}\text{-Ca(DME)(OTf)}]^{2+}$ and $[\mathbf{9}\text{-Ca(OH}_2)_3]^{3+}$.

donors in L has shifted from bridging to terminal, and each manganese center is coordinated by a single pyridyl donor and κ_2-bridging acetate groups (Figure 10a). The Ca^{2+} center is seven-coordinate with a THF molecule in the apical position. Compound **11**-Ca represents the first accurate model of the cubane subsite of the OEC; this discrete cluster shows that rational synthetic methodologies can be developed toward accessing models of one of the most complex inorganic active sites known in biology. A comparison of the structure of **11**-Ca to EXAFS and XRD studies of the OEC core (Figure 10b) shows that the Mn−Mn and Mn−Ca distances are similar; the Mn−Mn distance in **11**-Ca is about 2.8 Å, longer than the 2.7 Å vectors observed by EXAFS,[28] but similar to the 2.8 and 2.9 Å Mn−Mn distances observed in the recent XRD structure.[36] The Ca−Mn distance in **11**-Ca is slightly shorter (3.23 Å) than the 3.3−3.5 Å distances calculated by EXAFS studies, likely because of the higher oxidation state and number of bridging acetate ligands in **11**-Ca.[28] The structure of **11**-Ca is also very similar to a related pivalate-supported $[Ca_2Mn_3O_4]$ cluster recently reported by Christou and co-workers containing a similar $[CaMn^{IV}{}_3O_4]$ subsite (Figure 10c).[105] In that example, the Ca−Mn distance is slightly longer (3.4 Å), with shorter Mn−Mn distances (2.73, 2.76, and 2.86 Å). The authors indicate that the asymmetry of the $[Ca_2Mn_3O_4]$ cluster distorts the structure, making it more analogous to the structure of the OEC. Finally, $CaMn_3O_4$ cubane subsites have been proposed in heterogeneous systems based on XAS studies (Figure 10d).[9] In these systems, EXAFS data revealed an average Mn−Mn distance of ca. 2.88 Å, again similar to the values observed for model compound **11**-Ca. On-going spectroscopic studies of **11**-Ca and related species are expected to provide insight relative to the properties of the OEC. Both synthetic systems displaying the $CaMn^{IV}{}_3O_4$ moiety show ferromagnetic coupling.[105,135]

2.3. Synthesis of Heterometallic Mn_3MO_x Complexes.

The rational, stepwise synthesis used in the present series of calcium/manganese mixed-metal oxido complexes allows for controlled, targeted changes to their structure and metal content. Given the outstanding questions regarding the role of Ca^{2+} in the OEC, synthetic targets that interrogate the effect of changing the nature of the redox-inactive metal in heterometallic clusters are of interest. Such clusters were targeted for both MMn_3O_2 and MMn_3O_4 motifs.

Under conditions similar to those for the synthesis of $[\mathbf{9}\text{-Ca(DME)(OTf)}]^{2+}$, Na^+-, Sr^{2+}-, and Y^{3+}-substituted dioxido clusters with the same $[MMn_3O_2]$ core can be formed by replacing $Ca(OTf)_2$ with the corresponding metal triflate precursor (Scheme 6).[134] Although the Sr^{2+}-substituted compound $[LSrMn^{III}{}_2Mn^{IV}O_2(OAc)_2(DME)(OTf)]^{2+}$ ($[\mathbf{9}\text{-Sr(DME)(OTf)}]^{2+}$) is analogous to the Ca^{2+} compound, the Y^{3+}-substituted dioxido complex was isolated in the more reduced $Mn^{III}{}_3$ state as

dx.doi.org/10.1021/ic402236f | Inorg. Chem. 2013, 52, 13833−13848

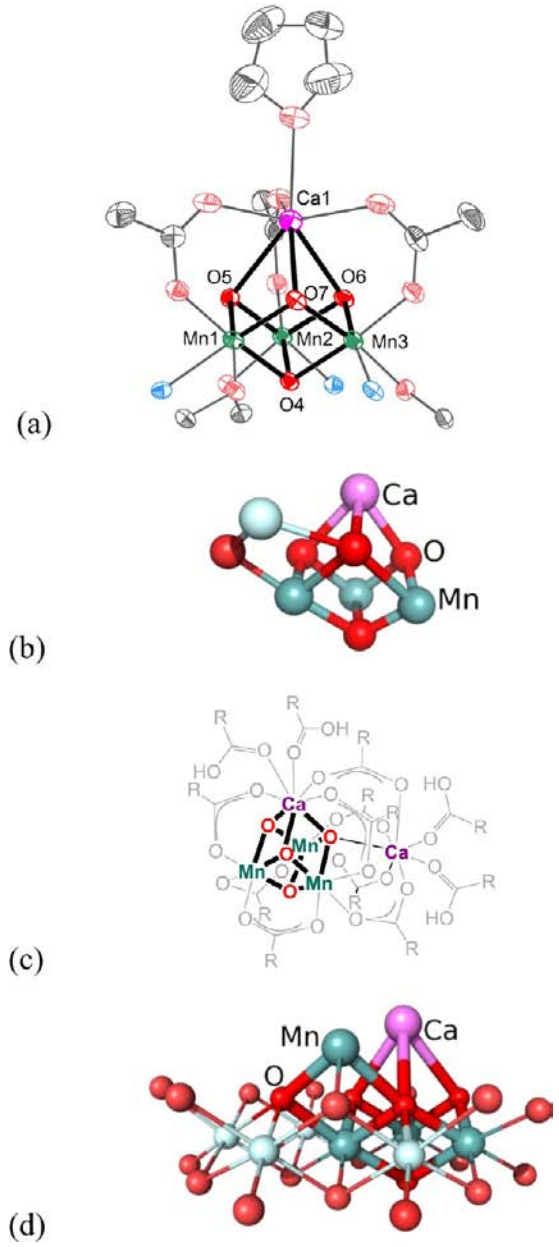

Figure 10. Comparison of $[CaMn_3O_4]$ structures. (a) Truncated view of the solid-state structure of **11**-Ca. (b) $CaMn_4O_5$ cluster of the OEC as found in the 1.9-Å-resolution structure,[36] with the $[CaMn_3O_4]$ subsite emphasized by thicker bonds. (c) $[Ca_2Mn_3O_4]$ cluster supported by pivalate ligands, with the $[CaMn_3O_4]$ subsite emphasized by bold bonds.[105] (d) Schematic drawing of one proposed structure of calcium-doped manganese oxide materials.[9]

$[LYMn^{III}_3O_2(OAc)_2(DME)(OTf)]^{2+}$ ($[\mathbf{10}\text{-Y(DME)(OTf)}]^{2+}$), and the Na^+-substituted complex was isolated as a dimer with sodium centers bridged through acetate oxygen atoms rather than coordinated by DME or triflate anions, $[LNaMn^{III}_2Mn^{IV}O_2(OAc)_2]_2^{4+}$ ($[\mathbf{9}\text{-Na}]_2^{4+}$). Analogously to the synthesis of the reduced complex $[\mathbf{10}\text{-Ca(DME)(OTf)}]^+$, the reduced Sr^{2+}-substituted complex $[LSrMn_3O_2(OAc)_2(DME)(OTf)]^+$ ($[\mathbf{10}\text{-Sr(DME)(OTf)}]^+$) was prepared by the addition of 1 equiv of $FeCp^*_2$ to $[\mathbf{9}\text{-Sr(DME)(OTf)}]^{2+}$. In a complementary synthetic route, the treatment of $[\mathbf{9}\text{-Ca(DME)(OTf)}]^{2+}$ with $Zn(OTf)_2$ leads to the zinc-capped dioxido cluster $[LZnMn_3O_2(OAc)_2(CH_3CN)][OTf]_3$ ($[\mathbf{9}\text{-Zn(CH}_3\text{CN)}]^{3+}$) via transmetalation.

Scheme 6. Synthesis of Heterometallic Dioxido Complexes

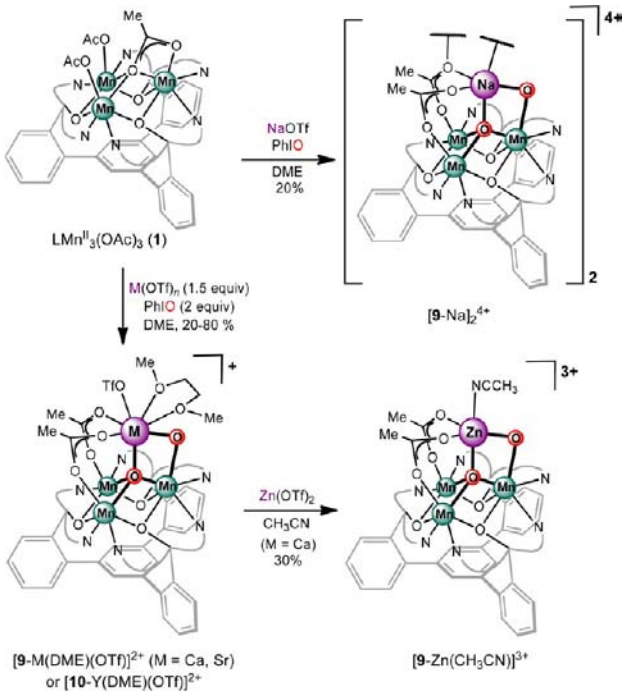

These complexes were all characterized by single-crystal XRD studies, and all maintain a similar $[MMn_3O_2]$ core structure with the same ligand L binding mode.

We also targeted a similar series of heterometallic tetraoxido clusters structurally related to the cubane subsite of the OEC.[136] The strontium-substituted complex $LSrMn^{IV}_3O_4(OAc)_3(DMF)$ (**11**-Sr) was prepared from **1**, $Sr(OTf)_2$, and KO_2 analogously to the synthesis of **11**-Ca (Scheme 7). Related complexes with other metals were not successfully isolated using this method, but transmetalation of **11**-Ca was found to be facile. As such, the corresponding $[MMn^{IV}_3O_4]$ complexes were prepared by the treatment of **11**-Ca with the metal triflate salt in DMF (Scheme 7; M = Zn^{2+}, Y^{3+}, Sc^{3+}). The Y^{3+}- and Sc^{3+}-substituted complexes are cationic because of the additional positive charge of the redox-inactive metal. The one-electron-reduced compound $LScMn^{III}Mn^{IV}_2O_4(OAc)_3(DMF)$ (**12**-Sc) was isolated by the reduction of $[\mathbf{11}\text{-Sc}][OTf]$ with 1 equiv of $FeCp^*_2$. Although the cubane structure is retained, the structural parameters show axial distortion diagnostic of manganese(III) due to population of a σ-antibonding orbital. All cubane complexes were characterized by XRD studies; they maintain the $[MMn_3O_4]$ cubane geometry of **11**-Ca.

Overall, the presented synthetic methodologies are very versatile. They have provided access to a variety of site-differentiated homo- and heterometallic tetranuclear clusters. With these series of compounds in hand, a variety of studies were performed to interrogate the properties of these clusters related to the OEC and proposed active sites of heterogeneous water oxidation catalysts.

3. INSIGHTS FROM STUDIES OF MANGANESE CLUSTERS

3.1. Mechanism of Oxidative Water Incorporation. Assembly of the OEC from reduced precursors requires oxidative water incorporation to generate the high-oxidation-state mixed-metal oxide cluster. Additionally, for each catalytic turnover of the water oxidation reaction, the substrate has to be coordinated to the

dx.doi.org/10.1021/ic402236f | Inorg. Chem. 2013, 52, 13833−13848

Scheme 7. Synthesis of Heterometallic Tetraoxido Cubane Complexes

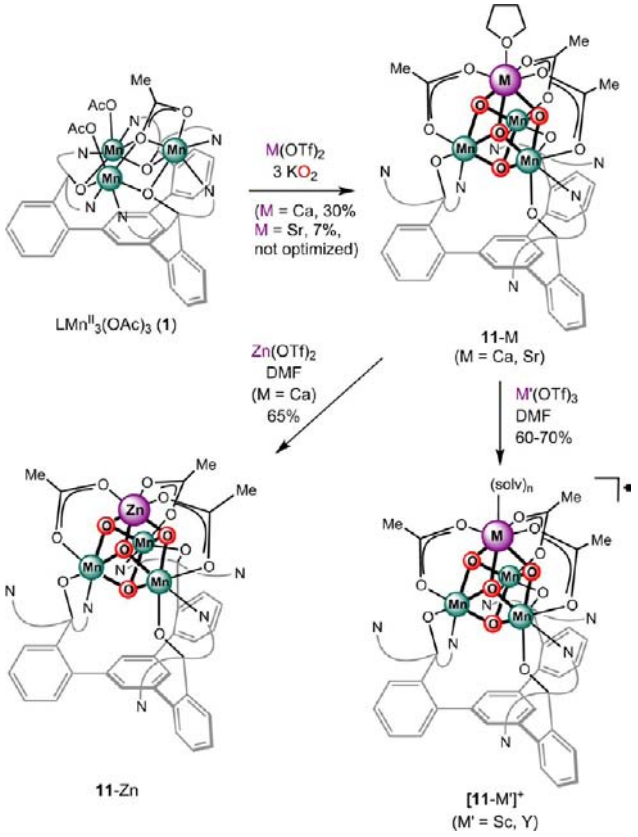

cluster and deprotonated (Figure 3). Site-differentiated clusters provide a convenient platform for studying the mechanism of oxidative water incorporation and oxygen-atom transfer.

During the formation of the OEC, called photoactivation,[137] water is deprotonated and incorporated into the manganese cluster at bridging oxido positions. Some proposals for the mechanism of the catalytic water oxidation cycle also suggest the oxidative incorporation of substrate water into bridging positions.[56,138] Substrate water exchange studies on the OEC revealed fast ($\geq$120 s^{-1} in S_2) and slow (2 s^{-1} in S_2) exchanging substrate waters.[139] These rates are faster than those observed in model systems containing μ_2- and μ_3-oxidos in dinuclear and tetranuclear manganese complexes.[140−142] Some use this distinction to argue that the substrate water molecules are terminally bound to manganese or calcium throughout the Kok cycle.[55,143] Others have argued that substrate water is indeed incorporated into a μ-oxido position but is in equilibrium between two sites in the S_1 and S_2 states (Scheme 8, top), thus affording this migrating oxido with a faster exchange rate than those observed in model complexes.[40,41,144]

We studied water exchange and the incorporation in homo- and heterometallic cubanes **2**, **11**-Ca, and [**11**-Sc]$^+$. Consistent with literature water exchange studies,[140−142] no exchange of $H_2{}^{18}O$ was observed over hours for these μ_3-oxide ligands.[135] To develop the mechanistic tools for studying the migration of oxide moieties within model clusters, we explored the possibility of interconversion between partial $Mn^{III}{}_4O_3$ cubane **6** and $Mn^{III}{}_2Mn^{IV}{}_2O_4$ cubane **2**. Because **2** and **6** differ by only an oxygen atom, we tested whether these could be interconverted by oxygen-atom acceptors (phosphines and thioethers),

Scheme 8. Proposed μ-Oxido Migration Equilibria between OEC Substates of S_1 and S_2 (Top)[40,41] and Proposed Mechanisms for Oxygen-Atom Transfer and Oxidative Water Incorporation That Depend on μ-Oxido Migration in Model Clusters (Bottom)[135]

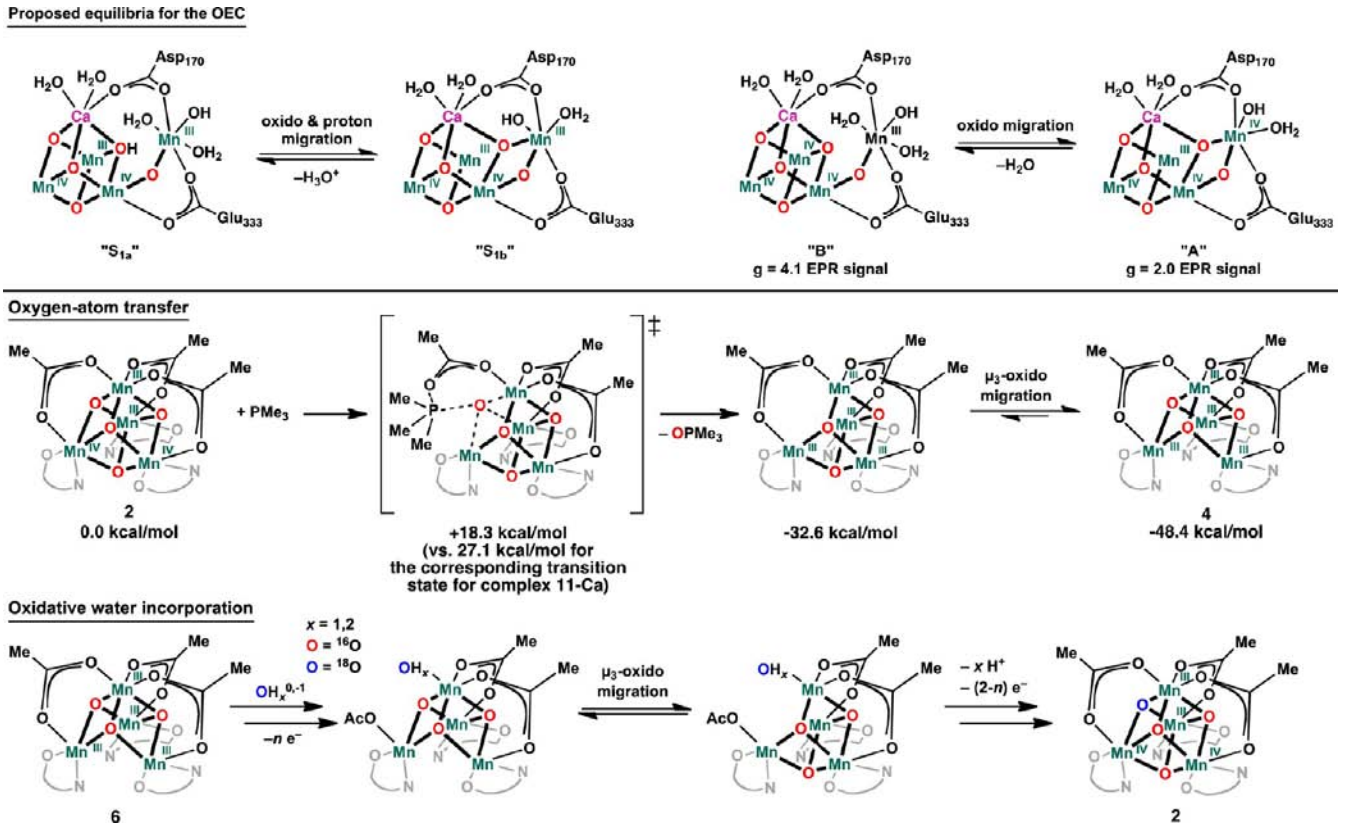

dx.doi.org/10.1021/ic402236f | Inorg. Chem. 2013, 52, 13833−13848

oxygen-atom donors (amine oxides and iodosobenzene), and oxidative water incorporation. The treatment of **2** with PMe_3 quantitatively afforded **6** (Scheme 8). The same reaction using PEt_3 is much slower, suggesting that sterics play an important role. For the reverse reaction, the treatment of **6** with PhIO afforded **2**. The heterometallic cubanes **11**-Ca and [**11**-Sc]$^+$ are stable to PMe_3, and no oxygen-atom transfer was observed by NMR spectroscopy. Because [**11**-Sc]$^+$ is more oxidizing than **2** and **11**-Ca, although for a one-electron-transfer process (vide infra), the difference in reactivity is consistent with kinetic rather than thermodynamic control for the oxygen-atom-transfer reaction. When ligand-exchange experiments with acetate-d_3 were performed with **2**, **11**-Ca, and [**11**-Sc]$^+$, the acetates scrambled much faster with **2** (statistical mixture in ca. 1 min) than **11**-Ca and [**11**-Sc]$^+$ (statistical mixture in ca. 1 h). This difference in rate is not surprising given the presence of manganese(III) centers in **2** that are labile because of population of a σ-antibonding orbital, while the heterometallic clusters **11**-Ca and [**11**-Sc]$^+$ have only manganese(IV) centers.

The reactivity of these cubanes was studied by quantum mechanics. As expected, PMe_3 attack at the bottom position was prohibitively high in energy because of steric interactions with ligand L. For **2**, a transition state was calculated where one acetate decoordinated from a bottom manganese to allow room for PMe_3 to approach a μ_3-oxido (Scheme 8, bottom). This transition state is ca. 9 kcal·mol^{-1} higher for **11**-Ca, consistent with the stronger Mn^{IV}–OAc bonds of **11**-Ca. The difference in the reactivity between the hetero- and homometallic clusters here shows that differences in the oxidation state can affect oxygen-atom-transfer chemistry indirectly by changing the ancillary ligand lability, in addition to changing the nature of the oxo moiety.

With the ability to interconvert **6** and **2** by oxygen-atom transfer, a detailed mechanistic study of water incorporation into the partial cubane **6** to form cubane **2** was undertaken. The addition of water, hydroxide, and a one-electron oxidant to **6** in THF/CH_3CN mixtures afforded **2** in ca. 95% purity (Scheme 8). Removal of any single reagent either shut down production of **2** or decreased the yield substantially. The present protocol mimics the biological incorporation of an oxido ligand into the OEC, and taking into account the oxidation states, it corresponds conceptually to the putative final steps of photoactivation, the conversion of S_{-1} to S_1.

An ^{18}O-labeling study was devised as a mechanistic probe that utilized the site differentiation given by the ligand framework. Labeled base and water ($NMe_4{}^{18}OH$ and $H_2{}^{18}O$) were utilized in the water incorporation conditions. Incorporation of ^{18}O into the cubane product (**2***) was observed by electrospray ionization mass spectrometry. Although the "bottom" oxido is missing in the partial cubane **6**, the isotopically labeled atom of **2*** could be located at any of the oxido positions in the cubane. The site of the label was interrogated by oxygen-atom transfer from **2*** to trimethylphosphine to generate **6**/**6*** and trimethylphosphine oxide. The various mechanisms of oxidative oxido incorporation into the cluster from water and oxygen-atom transfer have distinct outcomes with respect to the ratio of isotopologues of products ($^{18}OPMe_3$ vs $^{16}OPMe_3$ and **6** vs **6***). Experimentally, a mixture of **6** and **6*** was observed, consistent with water incorporation and phosphine attack at one of the three top oxygen atoms. Water is likely incorporated at the top position, although unselective incorporation cannot be ruled out because this would also form a mixture of **6** and **6***. Nevertheless, the pathways consistent with the experimental outcome all require migration of oxido ligands within the cluster during the process of oxidative water incorporation. This provides a model compound analogue for the proposed μ-oxido migration equilibria for the OEC (Scheme 8, top).[40,41]

3.2. Effects of Redox-Inactive Ions on Cluster Redox Potentials. Redox-inactive ions affect electron-transfer rates and potentials in small-molecule monometallic complexes as well as biological and synthetic electron-transfer reactions (vide supra).[106,112,113,115,116,145–147] Additionally, chemical reactions such as hydrogen- and oxygen-atom transfer and O_2 reduction are significantly influenced by the presence of redox-inactive metals.[104,113,117,148]

Access to the two series of heterometallic manganese oxido complexes with isostructural dioxido and tetraoxido cores described in sections 2.2 and 2.3 provides a method of probing the effect of the redox-inactive metal on the physical properties of multimetallic clusters. The ability of the framework to accommodate monocationic, dicationic, and tricationic metal ions within the same positions of the clusters allows variation of a wide range of metal properties, including the ionic radius, charge, and Lewis acidity.

The potentials of the quasi-reversible $[Mn^{III}{}_2Mn^{IV}O_2]$/$[MMn^{III}{}_3O_2]$ couples of the $[MMn_3O_2]$ complexes **9** and **10** (M = Na^+, Sr^{2+}, Ca^{2+}, Zn^{2+}, Y^{3+}) were measured using cyclic voltammetry. A significant shift of the potential was observed upon substitution of the redox-inactive metal; for example, the redox potential measured for the $[YMn_3O_2]$ cluster is 420 mV versus the ferrocene/ferrocenium couple (Fc/Fc$^+$), while that of the $[SrMn_3O_2]$ compound is −70 mV vs Fc/Fc$^+$, a difference of nearly 0.5 V. Although redox-inactive metals of higher charge lead to more oxidizing clusters, this shift in the potential cannot be attributed to only an electrostatic effect, which was previously invoked for shifts in the reduction potential of oxo-bridged manganese dimers supported by crown-ether-modified ligands with associated alkali and alkaline-earth metals.[149] The potential measured for the $[ZnMn_3O_2]$ cluster is more than 200 mV more positive than that of the strontium-substituted cluster, although both contain dicationic apical metals.

When the redox potentials are plotted against the pK_a values of the redox-inactive M(aqua)$^{n+}$ ion, used here as a measure of the Lewis acidity, a linear dependence is observed (Figure 11),

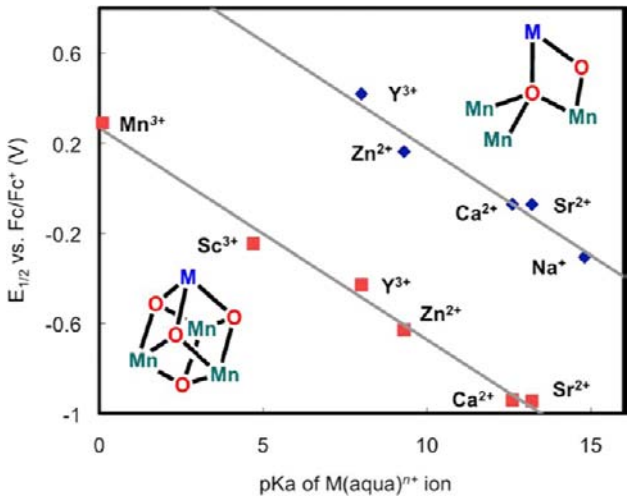

Figure 11. Reduction potentials of heterometallic trimanganese tetraoxido (red squares) and dioxido (blue diamonds) clusters plotted against the pK_a values of the corresponding metal(aqua)$^{n+}$ ion, used as a measure of the Lewis acidity.[136] Reproduced from ref 136.

dx.doi.org/10.1021/ic402236f | Inorg. Chem. 2013, 52, 13833−13848

with the potential shifting by ca. 90 mV per pK_a unit. This effect likely results from the interaction of the oxido moieties with redox-inactive metals versus manganese centers. The stronger Lewis acid draws more electron density from the oxido ligands, destabilizing the higher-oxidation-state manganese centers and shifting the potential to more positive values. The effect of the redox-inactive metals supports previous proposals that Ca^{2+}, in addition to serving as a site for water or hydroxide coordination in the OEC, may modulate the potential of the manganese cluster for water oxidation.[26,66,150] It is important to note that the potentials of the Ca^{2+}- and Sr^{2+}-substituted dioxido complexes are the same, which correlates with the observation that the OEC is active only with these two redox-inactive metals.[52,57] In other studies, the addition of redox-inactive metals has been shown to affect the rates of electron transfer involving organic or inorganic substrates.[145,146] Recently, the groups of Fukuzumi and Nam reported the rates of reduction of iron−oxo complexes to depend in a linear fashion on the Lewis acidity of redox-inactive additives.[115,116] This kinetic effect represents another consequence of association of the redox-inactive metal with transition-metal oxo species.

The reduction potentials of the $[MMn_3O_4]$ cubane clusters **11**-M (M = Sr^{2+}, Ca^{2+}, Zn^{2+}, Y^{3+}, Sc^{3+}) were measured using cyclic voltammetry to determine whether a dependence on the metal-ion Lewis acidity could be observed for a different structural series of heterometallic manganese oxido clusters (Figure 12).[136] These

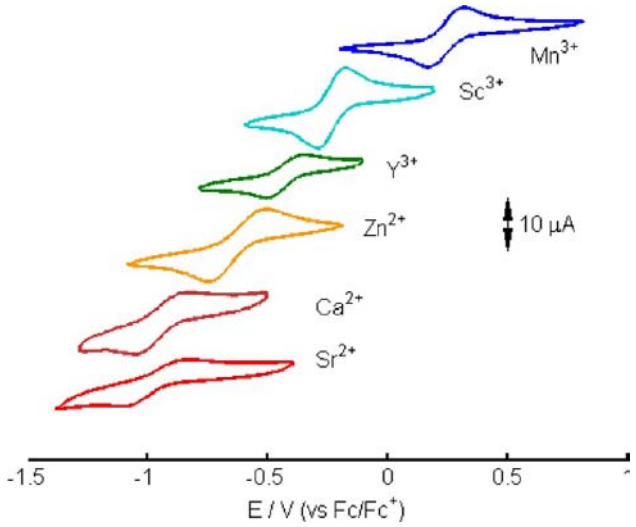

Figure 12. Cyclic voltammograms of the $[MMn^{IV}{}_3O_4]/[MMn^{III}Mn^{IV}{}_2O_4]$ couples of *N*,*N*-dimethylacetamide solutions of MMn_3O_4 complexes at a scan rate of 100 mV·s^{-1}. Potentials are referenced to the Fc/Fc$^+$ couple. Reproduced from ref 136.

complexes are also more structurally similar to the OEC and display higher oxidation states and oxido contents. Again, the reduction potentials shift significantly with the nature of the fourth metal. The charge of the cation is clearly not the single influencing factor because the Zn^{2+} species has a significantly more positive potential than the Ca^{2+} and Sr^{2+} cubanes, and the Y^{3+}, Sc^{3+}, and Mn^{3+} complexes are all separated by more than 200 mV each. A linear correlation is observed again between the redox potentials of the $[MMn^{IV}{}_3O_4]/[MMn^{III}Mn^{IV}{}_2O_4]$ couple and the Lewis acidity of the redox-inactive metal M (Figure 11). With the inclusion of the potential of the $[Mn^{III}Mn^{IV}{}_3O_4]/[Mn^{III}{}_2Mn^{IV}{}_2O_4]$ couple, measured from cyclic voltammetry of **2**, the redox potentials of the structurally similar $[MMn_3O_4]$ clusters (M = Sr^{2+}, Ca^{2+}, Zn^{2+}, Y^{3+}, Sc^{3+}, Mn^{3+}) span over 1.2 V, corresponding to a 28 kcal·mol^{-1} change in energy. This large difference in the redox potential, effected by simple substitution, is consistent with observations that the addition of Lewis acids to both inorganic and organic compounds can have a large effect on the reactivity and kinetic properties.[104,113−117,145,146,148]

$SrMn_3O_4$ and $CaMn_3O_4$ have very similar reduction potentials, analogous to the MMn_3O_2 species. Borovik's Ca−(μ-OH)−M and Sr−(μ-OH)−M complexes have similar potentials as well.[106] Given the expected large effect on the cluster potential by other metals (Figure 11), these results suggest that Sr^{2+} restores partial activity in calcium-depleted PSII because the potentials of the resulting clusters are similar. The difference in the catalytic activity between the Ca^{2+} and Sr^{2+} OECs may be caused by other subtle effects, such as the different levels of activation of a coordinated water substrate for O−O bond formation.

Although the $[MMn_3O_4]$ and $[MMn_3O_2]$ clusters differ significantly in the oxidation state, geometry, and coordination mode of the ligand framework, the linear correlations between the redox potential and Lewis acidity of both series of compounds have the same slope (Figure 11). This observation suggests that the dependence of the reduction potential on the Lewis acidity may be a general phenomenon for mixed-metal oxide clusters. Notably, the intercepts of the two lines differ by ca. 900 mV, with the $[MMn^{IV}{}_3O_4]$ complexes having more negative reduction potentials than the corresponding $[MMn^{IV}Mn^{III}{}_2O_2]$ despite the lower oxidation state of the dioxide species. This large difference in potential is likely due to the lower oxide content in compound **9** versus compound **11**, pointing to a different path of tuning the cluster potential by varying the number of oxide moieties. The synthetic $CaMn_3$ clusters ($[CaMn^{IV}{}_3O_4]$ and $[CaMn^{III}{}_2Mn^{IV}O_2]$) have potentials negative of the thermodynamic potential for water oxidation, probably because of a combination of the higher oxidation state, different Mn/O ratio, and nature of the ancillary ligands for the OEC.

Beyond insights related to the OEC, the systematic effects observed for redox-inactive metals in clusters of different structures suggest that the redox chemistry of other materials could be tuned quantitatively based on the same approach. For isostructural catalytic sites, the reduction potential could be affected by the simple replacement of the redox-inactive metal toward lowering overpotentials or making a reaction thermodynamically favorable. The same principles may be applicable to larger clusters or other materials with strong direct or indirect interactions between different metals. In the context of mixed-metal oxides, for example, applications include water oxidation and O_2 reduction catalysis and battery materials.[15,16,20−23]

4. CONCLUSIONS AND OUTLOOK

A synthetic methodology with unprecedented structural control was developed for the synthesis of manganese oxido complexes that model the OEC of PSII and proposed sites of catalysis in mixed-metal oxide catalysts for water oxidation. A stepwise oxidative functionalization strategy was employed by the controlled addition of a metal source and an oxidant to a trimanganese(II) complex supported by a rigid multinucleating framework. Tetramanganese clusters of varying oxide content, as well as heterometallic tetranuclear clusters containing different redox-inactive metals, were isolated in several oxidation states. These structural models have provided insight related to the properties and function of the OEC. The site differentiation of the metals in these clusters have allowed for isotopic-labeling studies to support

dx.doi.org/10.1021/ic402236f | *Inorg. Chem.* 2013, 52, 13833−13848

pathways of oxide migration within the cluster, reminiscent of proposals for the OEC. Electrochemical studies of an isostructural series of manganese dioxide and tetraoxido clusters revealed a linear dependence of the redox potentials of the clusters on the Lewis acidity of the incorporated redox-inactive metal. The effect of the Lewis acidity of a redox-inactive metal is remarkably high, shifting the potential over a range of more than 1 V. These results point to a role of Ca^{2+} in PSII for tuning the reduction potential of the catalytic site. Additionally, the effects discovered in these studies may be applicable to a variety of catalytic and functional materials with discrete or extended structure.

Future work includes the synthesis of models of the full OEC by functionalizing the $[CaMn_3O_4]$ cubane with a fourth manganese center for greater similarity to the structure of the biological $[CaMn_4O_5]$ cluster. Spectroscopic studies are ongoing to complement investigations of the biological system and to provide insight into the electronic structure of these compounds. Related heterometallic complexes of other transition metals supported by this and other ligand frameworks are of interest to test the generality of the reactivity and electrochemical studies beyond manganese. Additionally, the study of mixed-transition-metal oxide clusters is an exciting area given the interesting properties emerging for heterogeneous metal oxides applied to water oxidation and oxygen reduction catalysis and to metal oxide battery materials. These studies are expected to afford a detailed understanding of the effect of the cluster structure on the reactivity related to O_2 chemistry in the biological and artificial systems: electron-transfer chemistry, oxygen-atom transfer, and ultimately O−O bond formation and cleavage. The synthetic methodologies described here are hoped to provide a stimulating precedent for the rational design and study of other complex clusters of practical and fundamental interest.

AUTHOR INFORMATION

Corresponding Author

*E-mail: agapie@caltech.edu.

Notes

The authors declare no competing financial interest.

Biographies

Emily Tsui received a S.B. from MIT in 2008, where she did undergraduate research in the groups of Professors Joseph Sadighi and Timothy Swager. She joined the Agapie group as a graduate student at Caltech in 2008, where she has studied the synthesis and reactivity of biomimetic heterometallic cluster complexes. Upon graduation, she plans to move to the University of Washington as a postdoctoral research associate. She has been awarded a NSF Graduate Research Fellowship (2008) and a Sandia Campus Executive Fellowship (2012).

Jacob Kanady graduated summa cum laude with a B.S. from the University of California, Irvine, in 2009. At UCI, he worked in the Vanderwal group on stereoselective dichlorination methodology. He joined the Agapie group as a graduate student at the California Institute of Technology in late 2009, where he has worked on synthesizing model complexes of the oxygen-evolving complex of photosystem II. His interests lie in the chemical transformations of alternative and fossil fuel energy systems, from both bioinorganic and heterogeneous catalysis points of view. He plans on continuing in academia with a postdoctoral position. He has been awarded the Dow Chemical Company Graduate Fellowship (2009), Rose Hills Grant (2010), and NSF Graduate Research Fellowship (2011).

Theodor Agapie received his B.S. degree from Massachusetts Institute of Technology in 2001, where he performed research under the mentorship of Prof. Christopher C. Cummins. He received his Ph.D. from California Institute of Technology in 2007 with Prof. John E. Bercaw. After postdoctoral studies with Prof. Michael A. Marletta at University of California, Berkeley, he returned to Caltech in 2009 to start his independent career as an assistant professor of chemistry. Research in the Agapie laboratory is in the general area of inorganic synthesis and catalyst design, with inspiration from biological systems. Multimetallic and metal−ligand cooperativity are targeted for facilitating transformations of small molecules and functionalized organic substrates, and redox chemistry. Agapie is particularly interested in the synthesis of metal complexes that display unusual chemical reactivity and offer insight into the function of complicated biological catalysts. He has been the recipient of several awards including the Searle Scholar

(2010), Sloan Fellowship (2012), NSF CAREER Award (2012), Dreyfus Environmental Chemistry Mentor (2012), Cottrell Scholar (2013), Stiefel Young Investigator Award (2013), and ACS Award in Pure Chemistry (2013).

■ ACKNOWLEDGMENTS

We thank the California Institute of Technology, the Searle Scholars Program, NSF CAREER Grant CHE-1151918, NIH R01 GM102687A (to T.A.), a Sandia Campus Executive Fellowship (to E.Y.T.), and NSF Graduate Fellowships (to E.Y.T. and J.S.K.) for financial support. We are grateful to collaborators for insightful discussions and to colleagues and co-workers for a stimulating environment in which to do science at Caltech.

■ REFERENCES

(1) Wydrzynski, T. J.; Satoh, K. *Photosystem II: The Light-Driven Water: Plastoquinone Oxidoreductase*; Springer: Dordrecht, The Netherlands, 2005; Vol. *22*.
(2) McEvoy, J. P.; Brudvig, G. W. *Chem. Rev.* **2006**, *106*, 4455.
(3) Brudvig, G. W. *Philos. Trans. R. Soc., B* **2008**, *363*, 1211.
(4) Joliot, P.; Barbieri, G.; Chabaud, R. *Photochem. Photobiol.* **1969**, *10*, 309.
(5) Kok, B.; Forbush, B.; Mcgloin, M. *Photochem. Photobiol.* **1970**, *11*, 457.
(6) Symes, M. D.; Surendranath, Y.; Lutterman, D. A.; Nocera, D. G. *J. Am. Chem. Soc.* **2011**, *133*, 5174.
(7) Risch, M.; Klingan, K.; Ringleb, F.; Chernev, P.; Zaharieva, I.; Fischer, A.; Dau, H. *ChemSusChem* **2012**, *5*, 542.
(8) Zaharieva, I.; Najafpour, M. M.; Wiechen, M.; Haumann, M.; Kurz, P.; Dau, H. *Energy Environ. Sci.* **2011**, *4*, 2400.
(9) Wiechen, M.; Zaharieva, I.; Dau, H.; Kurz, P. *Chem. Sci.* **2012**.
(10) Zaharieva, I.; Chernev, P.; Risch, M.; Klingan, K.; Kohlhoff, M.; Fischer, A.; Dau, H. *Energy Environ. Sci.* **2012**, *5*, 7081.
(11) Najafpour, M. M.; Ehrenberg, T.; Wiechen, M.; Kurz, P. *Angew. Chem., Int. Ed.* **2010**, *49*, 2233.
(12) Najafpour, M. M.; Nayeri, S.; Pashaei, B. *Dalton Trans.* **2011**, *40*, 9374.
(13) Shevela, D.; Koroidov, S.; Najafpour, M. M.; Messinger, J.; Kurz, P. *Chem.—Eur. J.* **2011**, *17*, 5415.
(14) Najafpour, M. M.; Pashaei, B.; Nayeri, S. *Dalton Trans.* **2012**, *41*, 4799.
(15) Suntivich, J.; May, K. J.; Gasteiger, H. A.; Goodenough, J. B.; Shao-Horn, Y. *Science* **2011**, *334*, 1383.
(16) Smith, R. D. L.; Prévot, M. S.; Fagan, R. D.; Zhang, Z.; Sedach, P. A.; Siu, M. K. J.; Trudel, S.; Berlinguette, C. P. *Science* **2013**, *340*, 60.
(17) Liang, Y.; Wang, H.; Zhou, J.; Li, Y.; Wang, J.; Regier, T.; Dai, H. *J. Am. Chem. Soc.* **2012**, *134*, 3517.
(18) Suntivich, J.; Gasteiger, H. A.; Yabuuchi, N.; Nakanishi, H.; Goodenough, J. B.; Shao-Horn, Y. *Nat. Chem.* **2011**, *3*, 546.
(19) Hamdani, M.; Singh, R. N.; Chartier, P. *Int. J. Electrochem. Sci.* **2010**, *5*, 556.
(20) Goodenough, J. B.; Kim, Y. *Chem. Mater.* **2009**, *22*, 587.
(21) Whittingham, M. S. *Chem. Rev.* **2004**, *104*, 4271.
(22) Reddy, M. V.; Subba Rao, G. V.; Chowdari, B. V. R. *Chem. Rev.* **2013**, *113*, 5364.
(23) Melot, B. C.; Tarascon, J. M. *Acc. Chem. Res.* **2013**, *46*, 1226.
(24) Kirby, J. A.; Robertson, A. S.; Smith, J. P.; Thompson, A. C.; Cooper, S. R.; Klein, M. P. *J. Am. Chem. Soc.* **1981**, *103*, 5529.
(25) Kirby, J. A.; Goodin, D. B.; Wydrzynski, T.; Robertson, A. S.; Klein, M. P. *J. Am. Chem. Soc.* **1981**, *103*, 5537.
(26) Yachandra, V. K.; Sauer, K.; Klein, M. P. *Chem. Rev.* **1996**, *96*, 2927.
(27) Sauer, K.; Yano, J.; Yachandra, V. *Photosynth. Res.* **2005**, *85*, 73.
(28) Yano, J.; Kern, J.; Sauer, K.; Latimer, M. J.; Pushkar, Y.; Biesiadka, J.; Loll, B.; Saenger, W.; Messinger, J.; Zouni, A.; Yachandra, V. K. *Science* **2006**, *314*, 821.
(29) Messinger, J.; Nugent, J. H. A.; Evans, M. C. W. *Biochemistry* **1997**, *36*, 11055.
(30) Messinger, J.; Robblee, J. H.; Yu, W. O.; Sauer, K.; Yachandra, V. K.; Klein, M. P. *J. Am. Chem. Soc.* **1997**, *119*, 11349.
(31) Peloquin, J. M.; Campbell, K. A.; Randall, D. W.; Evanchik, M. A.; Pecoraro, V. L.; Armstrong, W. H.; Britt, R. D. *J. Am. Chem. Soc.* **2000**, *122*, 10926.
(32) Dismukes, G. C.; Siderer, Y. *FEBS Lett.* **1980**, *121*, 78.
(33) Dismukes, G. C.; Siderer, Y. *Proc. Natl. Acad. Sci.—Biol.* **1981**, *78*, 274.
(34) Dismukes, G. C.; Ferris, K.; Watnick, P. *Photobiochem. Photobiophys.* **1982**, *3*, 243.
(35) Ferreira, K. N.; Iverson, T. M.; Maghlaoui, K.; Barber, J.; Iwata, S. *Science* **2004**, *303*, 1831.
(36) Umena, Y.; Kawakami, K.; Shen, J. R.; Kamiya, N. *Nature* **2011**, *473*, 55.
(37) Luber, S.; Rivalta, I.; Umena, Y.; Kawakami, K.; Shen, J.-R.; Kamiya, N.; Brudvig, G. W.; Batista, V. S. *Biochemistry* **2011**, *50*, 6308.
(38) Ames, W.; Pantazis, D. A.; Krewald, V.; Cox, N.; Messinger, J.; Lubitz, W.; Neese, F. *J. Am. Chem. Soc.* **2011**, *133*, 19743.
(39) Yano, J.; Kern, J.; Irrgang, K.-D.; Latimer, M. J.; Bergmann, U.; Glatzel, P.; Pushkar, Y.; Biesiadka, J.; Loll, B.; Sauer, K.; Messinger, J.; Zouni, A.; Yachandra, V. K. *Proc. Natl. Acad. Sci. U.S.A.* **2005**, *102*, 12047.
(40) Kusunoki, M. *J. Photochem. Photobiol. B* **2011**, *104*, 100.
(41) Pantazis, D. A.; Ames, W.; Cox, N.; Lubitz, W.; Neese, F. *Angew. Chem., Int. Ed.* **2012**, *51*, 9935.
(42) Siegbahn, P. E. M. *Chem.—Eur. J.* **2008**, *14*, 8290.
(43) Grundmeier, A.; Dau, H. *Biochim. Biophys. Acta, Bioenerg.* **2012**, *1817*, 88.
(44) Messinger, J.; Badger, M.; Wydrzynski, T. *Proc. Natl. Acad. Sci. U.S.A.* **1995**, *92*, 3209.
(45) Hillier, W.; Messinger, J.; Wydrzynski, T. *Biochemistry* **1998**, *37*, 16908.
(46) Rapatskiy, L.; Cox, N.; Savitsky, A.; Ames, W. M.; Sander, J.; Nowaczyk, M. M.; Rögner, M.; Boussac, A.; Neese, F.; Messinger, J.; Lubitz, W. *J. Am. Chem. Soc.* **2012**, *134*, 16619.
(47) Dasgupta, J.; van Willigen, R. T.; Dismukes, G. C. *Phys. Chem. Chem. Phys.* **2004**, *6*, 4793.
(48) Vincent, J. B.; Christou, G. *Inorg. Chim. Acta* **1987**, *136*, L41.
(49) Brudvig, G. W.; Crabtree, R. H. *Proc. Natl. Acad. Sci. U.S.A.* **1986**, *83*, 4586.
(50) Pecoraro, V. L.; Baldwin, M. J.; Caudle, M. T.; Hsieh, W. Y.; Law, N. A. *Pure Appl. Chem.* **1998**, *70*, 925.
(51) Vrettos, J. S.; Limburg, J.; Brudvig, G. W. *Biochim. Biophys. Acta, Bioenerg.* **2001**, *1503*, 229.
(52) Vrettos, J. S.; Stone, D. A.; Brudvig, G. W. *Biochemistry* **2001**, *40*, 7937.
(53) Siegbahn, P. E. M.; Crabtree, R. H. *J. Am. Chem. Soc.* **1999**, *121*, 117.
(54) Siegbahn, P. E. M. *Philos. Trans. R. Soc., B* **2008**, *363*, 1221.
(55) Sproviero, E. M.; Gascón, J. A.; McEvoy, J. P.; Brudvig, G. W.; Batista, V. S. *J. Am. Chem. Soc.* **2008**, *130*, 3428.
(56) Siegbahn, P. E. M. *Acc. Chem. Res.* **2009**, *42*, 1871.
(57) Ghanotakis, D. F.; Babcock, G. T.; Yocum, C. F. *FEBS Lett.* **1984**, *167*, 127.
(58) Boussac, A.; Zimmermann, J. L.; Rutherford, A. W. *Biochemistry* **1989**, *28*, 8984.
(59) Yocum, C. F. *Biochim. Biophys. Acta, Bioenerg.* **1991**, *1059*, 1.
(60) Yocum, C. F. *Coord. Chem. Rev.* **2008**, *252*, 296.
(61) Boussac, A.; Rutherford, A. W. *Biochemistry* **1988**, *27*, 3476.
(62) Pushkar, Y.; Yano, J.; Sauer, K.; Boussac, A.; Yachandra, V. K. *Proc. Natl. Acad. Sci. U.S.A.* **2008**, *105*, 1879.
(63) Cox, N.; Rapatskiy, L.; Su, J.-H.; Pantazis, D. A.; Sugiura, M.; Kulik, L.; Dorlet, P.; Rutherford, A. W.; Neese, F.; Boussac, A.; Lubitz, W.; Messinger, J. *J. Am. Chem. Soc.* **2011**, *133*, 3635.
(64) Lee, C.-I.; Lakshmi, K. V.; Brudvig, G. W. *Biochemistry* **2007**, *46*, 3211.

(65) Yachandra, V. K.; Yano, J. *J. Photochem. Photobiol. B* **2011**, *104*, 51.
(66) Riggs-Gelasco, P. J.; Mei, R.; Ghanotakis, D. F.; Yocum, C. F.; Penner-Hahn, J. E. *J. Am. Chem. Soc.* **1996**, *118*, 2400.
(67) Lohmiller, T.; Cox, N.; Su, J.-H.; Messinger, J.; Lubitz, W. *J. Biol. Chem.* **2012**, *287*, 24721.
(68) Kanan, M. W.; Yano, J.; Surendranath, Y.; Dincă, M.; Yachandra, V. K.; Nocera, D. G. *J. Am. Chem. Soc.* **2010**, *132*, 13692.
(69) Wieghardt, K. *Angew. Chem., Int. Ed. Engl.* **1989**, *28*, 1153.
(70) Cady, C. W.; Crabtree, R. H.; Brudvig, G. W. *Coord. Chem. Rev.* **2008**, *252*, 444.
(71) Sproviero, E. M.; Gascón, J. A.; McEvoy, J. P.; Brudvig, G. W.; Batista, V. S. *Coord. Chem. Rev.* **2008**, *252*, 395.
(72) Christou, G. *Acc. Chem. Res.* **1989**, *22*, 328.
(73) Pecoraro, V. L.; Baldwin, M. J.; Gelasco, A. *Chem. Rev.* **1994**, *94*, 807.
(74) Manchanda, R.; Brudvig, G. W.; Crabtree, R. H. *Coord. Chem. Rev.* **1995**, *144*, 1.
(75) Yagi, M.; Kaneko, M. *Chem. Rev.* **2000**, *101*, 21.
(76) Mukhopadhyay, S.; Mandal, S. K.; Bhaduri, S.; Armstrong, W. H. *Chem. Rev.* **2004**, *104*, 3981.
(77) Wu, A. J.; Penner-Hahn, J. E.; Pecoraro, V. L. *Chem. Rev.* **2004**, *104*, 903.
(78) Mullins, C. S.; Pecoraro, V. L. *Coord. Chem. Rev.* **2008**, *252*, 416.
(79) Plaksin, P. M.; Stoufer, R. C.; Mathew, M.; Palenik, G. J. *J. Am. Chem. Soc.* **1972**, *94*, 2121.
(80) Cooper, S. R.; Calvin, M. *J. Am. Chem. Soc.* **1977**, *99*, 6623.
(81) Cooper, S. R.; Dismukes, G. C.; Klein, M. P.; Calvin, M. *J. Am. Chem. Soc.* **1978**, *100*, 7248.
(82) Kirby, J. A.; Robertson, A. S.; Smith, J. P.; Thompson, A. C.; Cooper, S. R.; Klein, M. P. *J. Am. Chem. Soc.* **1981**, *103*, 5529.
(83) Dismukes, G. C.; Siderer, Y. *Proc. Natl. Acad. Sci. U.S.A.* **1981**, *78*, 274.
(84) Guiles, R. D.; Zimmermann, J. L.; McDermott, A. E.; Yachandra, V. K.; Cole, J. L.; Dexheimer, S. L.; Britt, R. D.; Wieghardt, K.; Bossek, U. *Biochemistry* **1990**, *29*, 471.
(85) Chan, M. K.; Armstrong, W. H. *J. Am. Chem. Soc.* **1991**, *113*, 5055.
(86) Chen, H.; Faller, J. W.; Crabtree, R. H.; Brudvig, G. W. *J. Am. Chem. Soc.* **2004**, *126*, 7345.
(87) Philouze, C.; Blondin, G.; Girerd, J.-J.; Guilhem, J.; Pascard, C.; Lexa, D. *J. Am. Chem. Soc.* **1994**, *116*, 8557.
(88) Limburg, J.; Brudvig, G. W.; Crabtree, R. H. *J. Am. Chem. Soc.* **1997**, *119*, 2761.
(89) Limburg, J.; Vrettos, J. S.; Liable-Sands, L. M.; Rheingold, A. L.; Crabtree, R. H.; Brudvig, G. W. *Science* **1999**, *283*, 1524.
(90) Limburg, J.; Vrettos, J. S.; Chen, H.; de Paula, J. C.; Crabtree, R. H.; Brudvig, G. W. *J. Am. Chem. Soc.* **2000**, *123*, 423.
(91) Vincent, J. B.; Christmas, C.; Chang, H. R.; Li, Q.; Boyd, P. D. W.; Huffman, J. C.; Hendrickson, D. N.; Christou, G. *J. Am. Chem. Soc.* **1989**, *111*, 2086.
(92) Vincent, J. B.; Christmas, C.; Huffman, J. C.; Christou, G.; Chang, H.-R.; Hendrickson, D. N. *J. Chem. Soc., Chem. Commun.* **1987**, *0*, 236.
(93) Li, Q.; Vincent, J. B.; Libby, E.; Chang, H.-R.; Huffman, J. C.; Boyd, P. D. W.; Christou, G.; Hendrickson, D. N. *Angew. Chem., Int. Ed. Engl.* **1988**, *27*, 1731.
(94) Ruettinger, W. F.; Campana, C.; Dismukes, G. C. *J. Am. Chem. Soc.* **1997**, *119*, 6670.
(95) Dismukes, G. C.; Brimblecombe, R.; Felton, G. A. N.; Pryadun, R. S.; Sheats, J. E.; Spiccia, L.; Swiegers, G. F. *Acc. Chem. Res.* **2009**, *42*, 1935.
(96) Brimblecombe, R.; Swiegers, G. F.; Dismukes, G. C.; Spiccia, L. *Angew. Chem., Int. Ed.* **2008**, *47*, 7335.
(97) Hocking, R. K.; Brimblecombe, R.; Chang, L.-Y.; Singh, A.; Cheah, M. H.; Glover, C.; Casey, W. H.; Spiccia, L. *Nat. Chem.* **2011**, *3*, 461.
(98) Wieghardt, K.; Bossek, U.; Gebert, W. *Angew. Chem., Int. Ed. Engl.* **1983**, *22*, 328.
(99) Dubé, C. E.; Wright, D. W.; Pal, S.; Bonitatebus, P. J., Jr.; Armstrong, W. H. *J. Am. Chem. Soc.* **1998**, *120*, 3704.
(100) Mishra, A.; Wernsdorfer, W.; Abboud, K. A.; Christou, G. *Chem. Commun.* **2005**, 54.
(101) Mishra, A.; Yano, J.; Pushkar, Y.; Yachandra, V. K.; Abboud, K. A.; Christou, G. *Chem. Commun.* **2007**, 1538.
(102) Hewitt, I. J.; Tang, J.-K.; Madhu, N. T.; Clerac, R.; Buth, G.; Anson, C. E.; Powell, A. K. *Chem. Commun.* **2006**, 2650.
(103) Nayak, S.; Nayek, H. P.; Dehnen, S.; Powell, A. K.; Reedijk, J. *Dalton Trans.* **2011**, *40*, 2699.
(104) Park, Y. J.; Ziller, J. W.; Borovik, A. S. *J. Am. Chem. Soc.* **2011**, *133*, 9258.
(105) Mukherjee, S.; Stull, J. A.; Yano, J.; Stamatatos, T. C.; Pringouri, K.; Stich, T. A.; Abboud, K. A.; Britt, R. D.; Yachandra, V. K.; Christou, G. *Proc. Natl. Acad. Sci. U.S.A.* **2012**, *109*, 2257.
(106) Park, Y. J.; Cook, S. A.; Sickerman, N. S.; Sano, Y.; Ziller, J. W.; Borovik, A. S. *Chem. Sci.* **2013**, *4*, 717.
(107) Mishra, A.; Pushkar, Y.; Yano, J.; Yachandra, V. K.; Wernsdorfer, W.; Abboud, K. A.; Christou, G. *Inorg. Chem.* **2008**, *47*, 1940.
(108) Kotzabasaki, V.; Siczek, M.; Lis, T.; Milios, C. J. *Inorg. Chem. Commun.* **2011**, *14*, 213.
(109) Koumousi, E. S.; Mukherjee, S.; Beavers, C. M.; Teat, S. J.; Christou, G.; Stamatatos, T. C. *Chem. Commun.* **2011**, *47*, 11128.
(110) Jerzykiewicz, L. B.; Utko, J.; Duczmal, M.; Sobota, P. *Dalton Trans.* **2007**, 825.
(111) Li, N.; Wang, M.; Ma, C.-B.; Hu, M.-Q.; Zhou, R.-W.; Chen, H.; Chen, C.-N. *Inorg. Chem. Commun.* **2010**, *13*, 730.
(112) Lacy, D. C.; Park, Y. J.; Ziller, J. W.; Yano, J.; Borovik, A. S. *J. Am. Chem. Soc.* **2012**, *134*, 17526.
(113) Chen, J.; Lee, Y.-M.; Davis, K. M.; Wu, X.; Seo, M. S.; Cho, K.-B.; Yoon, H.; Park, Y. J.; Fukuzumi, S.; Pushkar, Y. N.; Nam, W. *J. Am. Chem. Soc.* **2013**, *135*, 6388.
(114) Yoon, H.; Lee, Y.-M.; Wu, X.; Cho, K.-B.; Sarangi, R.; Nam, W.; Fukuzumi, S. *J. Am. Chem. Soc.* **2013**, *135*, 9186.
(115) Fukuzumi, S.; Morimoto, Y.; Kotani, H.; Naumov, P.; Lee, Y. M.; Nam, W. *Nat. Chem.* **2010**, *2*, 756.
(116) Morimoto, Y.; Kotani, H.; Park, J.; Lee, Y. M.; Nam, W.; Fukuzumi, S. *J. Am. Chem. Soc.* **2011**, *133*, 403.
(117) Leeladee, P.; Baglia, R. A.; Prokop, K. A.; Latifi, R.; de Visser, S. P.; Goldberg, D. P. *J. Am. Chem. Soc.* **2012**, *134*, 10397.
(118) Stack, T. D. P.; Holm, R. H. *J. Am. Chem. Soc.* **1987**, *109*, 2546.
(119) Venkateswara Rao, P.; Holm, R. H. *Chem. Rev.* **2003**, *104*, 527.
(120) Stack, T. D. P.; Holm, R. H. *J. Am. Chem. Soc.* **1988**, *110*, 2484.
(121) Ciurli, S.; Carrie, M.; Weigel, J. A.; Carney, M. J.; Stack, T. D. P.; Papaefthymiou, G. C.; Holm, R. H. *J. Am. Chem. Soc.* **1990**, *112*, 2654.
(122) Zhou, J.; Raebiger, J. W.; Crawford, C. A.; Holm, R. H. *J. Am. Chem. Soc.* **1997**, *119*, 6242.
(123) Stamatatos, T. C.; Efthymiou, C. G.; Stoumpos, C. C.; Perlepes, S. P. *Eur. J. Inorg. Chem.* **2009**, *2009*, 3361.
(124) Tsui, E. Y.; Day, M. W.; Agapie, T. *Angew. Chem., Int. Ed.* **2011**, *50*, 1668.
(125) Tsui, E. Y.; Kanady, J. S.; Day, M. W.; Agapie, T. *Chem. Commun.* **2011**, *47*, 4189.
(126) Kanady, J. S.; Tsui, E. Y.; Day, M. W.; Agapie, T. *Science* **2011**, *333*, 733.
(127) Wang, S.; Huffman, J. C.; Folting, K.; Streib, W. E.; Lobkovsky, E. B.; Christou, G. *Angew. Chem., Int. Ed. Engl.* **1991**, *30*, 1672.
(128) Wang, S.; Tsai, H.-L.; Hagen, K. S.; Hendrickson, D. N.; Christou, G. *J. Am. Chem. Soc.* **1994**, *116*, 8376.
(129) Aubin, S. M. J.; Wemple, M. W.; Adams, D. M.; Tsai, H.-L.; Christou, G.; Hendrickson, D. N. *J. Am. Chem. Soc.* **1996**, *118*, 7746.
(130) Aromi, G.; Wemple, M. W.; Aubin, S. J.; Folting, K.; Hendrickson, D. N.; Christou, G. *J. Am. Chem. Soc.* **1998**, *120*, 5850.
(131) Aliaga-Alcalde, N.; Edwards, R. S.; Hill, S. O.; Wernsdorfer, W.; Folting, K.; Christou, G. *J. Am. Chem. Soc.* **2004**, *126*, 12503.
(132) Kanady, J. S.; Tran, R.; Stull, J. A.; Lu, L.; Stich, T. A.; Day, M. W.; Yano, J.; Britt, R. D.; Agapie, T. *Chem. Sci.* **2013**, *4*, 3986−3996.

(133) Caudle, M. T.; Pecoraro, V. L. *J. Am. Chem. Soc.* **1997**, *119*, 3415.
(134) Tsui, E. Y.; Tran, R.; Yano, J.; Agapie, T. *Nat. Chem.* **2013**, *5*, 293.
(135) Kanady, J. S.; Mendoza-Cortes, J. L.; Tsui, E. Y.; Nielsen, R. J.; Goddard, W. A.; Agapie, T. *J. Am. Chem. Soc.* **2013**, *135*, 1073.
(136) Tsui, E. Y.; Agapie, T. *Proc. Natl. Acad. Sci. U.S.A.* **2013**, *110*, 10084.
(137) Cheniae, G. M.; Martin, I. F. *Biochem. Biophys. Res. Commun.* **1967**, *28*, 89.
(138) Siegbahn, P. E. M. *Phys. Chem. Chem. Phys.* **2012**, *14*, 4849.
(139) Hillier, W.; Wydrzynski, T. *Phys. Chem. Chem. Phys.* **2004**, *6*, 4882.
(140) Tagore, R.; Chen; Crabtree, R. H.; Brudvig, G. W. *J. Am. Chem. Soc.* **2006**, *128*, 9457.
(141) Tagore, R.; Crabtree, R. H.; Brudvig, G. W. *Inorg. Chem.* **2007**, *46*, 2193.
(142) Ohlin, C. A.; Brimblecombe, R.; Spiccia, L.; Casey, W. H. *Dalton Trans.* **2009**, *0*, 5278.
(143) Pecoraro, V. L.; Hsieh, W. Y. In *Manganese and Its Role in Biological Systems*; Sigel, A., Sigel, H., Eds.; Marcel Dekker, Inc.: New York, 2000; Vol. *37*, p 429.
(144) Siegbahn, P. E. M. *J. Am. Chem. Soc.* **2013**, *135*, 9442.
(145) Fukuzumi, S. In *Progress in Inorganic Chemistry*; Karlin, K. D., Ed.; John Wiley & Sons Inc.: New York, 2009; Vol. *56*, p 49.
(146) Fukuzumi, S.; Ohkubo, K. *Coord. Chem. Rev.* **2010**, *254*, 372.
(147) Fukuzumi, S.; Ohkubo, K. *Chem.—Eur. J.* **2000**, *6*, 4532.
(148) Park, J.; Morimoto, Y.; Lee, Y. M.; Nam, W.; Fukuzumi, S. *J. Am. Chem. Soc.* **2011**, *133*, 5236.
(149) Horwitz, C. P.; Ciringh, Y. *Inorg. Chim. Acta* **1994**, *225*, 191.
(150) Haumann, M.; Junge, W. *Biochim. Biophys. Acta, Bioenerg.* **1999**, *1411*, 121.